



Original article

Design, synthesis and 3D-QSAR analysis of novel 2-hydrazinyl-4-morpholinthieno[3,2-*d*]pyrimidine derivatives as potential antitumor agentsWufu Zhu^{a,b}, Yajing Liu^a, Xin Zhai^a, Xiao Wang^a, Yan Zhu^a, Di Wu^a, Hongyu Zhou^a, Ping Gong^a, Yanfang Zhao^{a,*}^aKey Laboratory of Original New Drugs Design and Discovery of Ministry of Education, Shenyang Pharmaceutical University, 103 Wenhua Road, Shenhe District, Shenyang 110016, PR China^bSchool of Pharmacy, Jiangxi Science and Technology Normal University, Nanchang, Jiangxi 330013, China

ARTICLE INFO

Article history:

Received 30 March 2012

Received in revised form

31 August 2012

Accepted 1 September 2012

Available online 10 September 2012

Keywords:

2-Hydrazinyl-4-morpholinthieno[3,2-*d*]pyrimidine

Synthesis

3D-QSAR

CoMFA

CoMSIA

Cytotoxic activity

ABSTRACT

A series of 2-hydrazinyl-4-morpholinthieno[3,2-*d*]pyrimidine derivatives were synthesized and evaluated for their cytotoxic activities against five cancer cell lines. Most of them exhibited moderate to significant cytotoxic activities and high-selectivity against one or more cell lines, and nearly all of them had higher potency than positive controls against MDA-MB-231 cell line. The most promising compound **15f** showed strong cytotoxic activities against H460, HT-29 and MDA-MB-231 cell lines, which were 1.7- to 66.5-folds more active than 2-(1*H*-indazol-4-yl)-6-((4-(methylsulfonyl)-1-piperazinyl)methyl)-4-(4-morpholinyl)thieno[3,2-*d*]pyrimidine (GDC-0941). To investigate the SARs of thieno[3,2-*d*]pyrimidine derivatives in more details, CoMFA ($q^2 = 0.436$, $r^2 = 0.937$) and CoMSIA ($q^2 = 0.706$, $r^2 = 0.947$) models on H460 cell line were established. The generated 3D-QSAR models can be used for further rational design of novel thienopyrimidines as highly potent and selective cytotoxic agents.

© 2012 Elsevier Masson SAS. All rights reserved.

1. Introduction

Despite efforts to prevent it, cancer remains a global killer, taking the lives of over 7 million people a year. What's more, deaths from cancer worldwide are projected to continue rising, with an estimated of 13.1 million in 2030 [1]. Although a range of antitumor drugs and therapies are available, drug resistance and adverse side effects are still serious problems. Therefore, the search for highly efficient and safe chemotherapeutic agents for treating cancer remains desirable.

Thienopyrimidine derivatives have attracted great attention over many years due to their broad bioactivities, including anti-tumor [2–5], antimicrobial [6], anti-inflammatory [7]. Of these active compounds, 4-morpholinthieno[3,2-*d*]pyrimidines have been reported to show marked antitumor activities with different biotargets and mechanisms [4,5,8]. For example, GDC-0941 (**1**, Fig. 1), which is a potent, selective, orally bioavailable inhibitor of PI3K, exerted antiproliferative effects against an array of human

tumor cell lines and is currently undergoing Phase I clinical trials [8–10]. Further optimization of GDC-0941 led to several backup clinical candidates with similar structures, such as GNE-477 (**2**, Fig. 1) [4], GNE-493 (**3a**, Fig. 1) [5], and GNE-490 (**3b**, Fig. 1) [5]. The structure–activity relationships (SARs) studies of these (pre)clinical compounds revealed that the morpholino substituted thieno[3,2-*d*]pyrimidine scaffolds play a key role in their anti-tumor activities [3–5,8].

However, nearly all of these reported 4-morpholinthieno[3,2-*d*]pyrimidines were obtained by introducing heterocyclic groups to the C-2 position of thienopyrimidine core through Suzuki Coupling reaction. The potential drawbacks of these derivatives are their strong structure rigidity, which may lead to a poor pharmacokinetic profile. Prompted by these observations, we speculated that compounds with flexible substituent at this position might possess equal even enhanced anti-tumor activity as well as an improved pharmacokinetic profile. It's worthwhile to search and discover some flexible molecules or functional groups. The flexible hydrazinyl group, which was widely used in the design of anticancer agents (**4** [11], **5** [12], **6** [13,14], Fig. 1), aroused our attention and was applied to the design of new compounds.

* Corresponding author. Tel./fax: +86 24 2398 6429.

E-mail address: yanfangzhao@126.com (Y. Zhao).

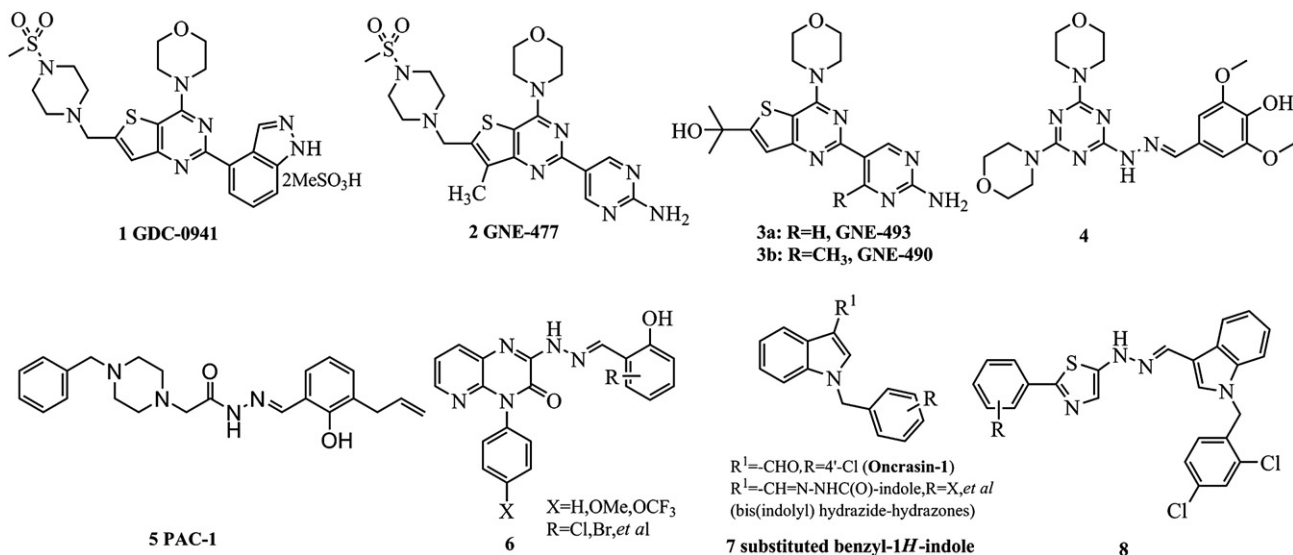


Fig. 1. Structures of 4-morpholinothieno[3,2-*d*]pyrimidines (GDC-0941,GNE-477,GNE-490,GNE-493), hydrazinyl group-containing compounds (**4**,PAC-1,**6**) and substituted heterocyclic compounds (**7,8**).

In view of above, we focused on the synthesis of novel 4-morpholinothieno[3,2-*d*]pyrimidines bearing flexible hydrazinyl groups at C2-position. Especially, we thought to introduce some *N*-benzyl heterocycles to the hydrazinyl groups. The *N*-benzyl indole moieties, which are frequently found in medicinal chemistry (Oncrasin-1 [15], bis(indolyl) hydrazide-hydrazones [16,17], **8** [18], Fig. 1), were introduced to afford compounds **15a–15o** (Fig. 2). And according to the theory of isostere principle, the indole ring was then replaced by benzimidazole moiety (**17a–17f**, Fig. 2). However, these benzimidazole-containing compounds (**17a–17f**) showed disappointing cytotoxic activities and thus we shifted our focus back to the *N*-benzyl indole series. To investigate the influences of C-6 position substituent to this series of derivatives, a hydroxy-isopropyl group that existed both in GNE-490 and GNE-493 was introduced to yield compounds **20c–20k** and **20p** (Fig. 2). These modifications might increase the bioavailability of the new compounds.

Herein we disclose the design, synthesis and cytotoxic activity of 2-hydrazinyl-4-morpholinothieno[3,2-*d*]pyrimidines against H460, HT-29, MDA-MB-231, U87MG and H1975 cancer cell lines.

Moreover, 3D-QSAR analysis employed by CoMFA and CoMSIA models on H460 cell line will be presented in this paper as well.

2. Chemistry

The preparation of target compounds **15a–15o**, **17a–17f**, **20c–20k** and **20p** was described in Scheme 1 [8]. The commercially available methyl 3-amino-2-thiophenecarboxylate **9** was condensed with urea at 190 °C for 2.5 h to give thienopyrimidinedione **10**. Chlorination of **10** with phosphorus oxychloride proceeded smoothly to **11** as a pale yellow solid. Regioselective nucleophilic displacement of the 4-chloride with morpholine, followed by hydrazinolysis gave access to the key intermediate **13**. Subsequently, **13** condensed with substituted benzyl-1*H*-indole-3-carbaldehydes **14a–14o** or 1-benzyl-1*H*-benzo[*d*]imidazole-2-carbaldehydes **16a–16f** to yield compounds **15a–15o** and **17a–17f**, respectively. On the other hand, compound **12** treated with *n*-BuLi and subsequently trapped with acetone to furnish a tertiary alcohol which was then used in a substitution reaction with NH₂NH₂·H₂O to generate another key intermediate **19**. Similarly, intermediate **19** condensed

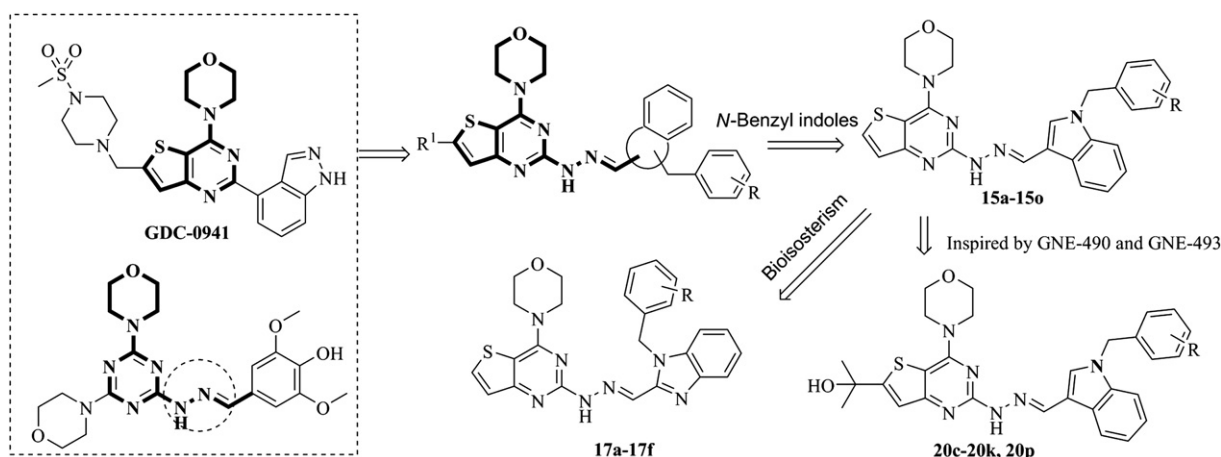
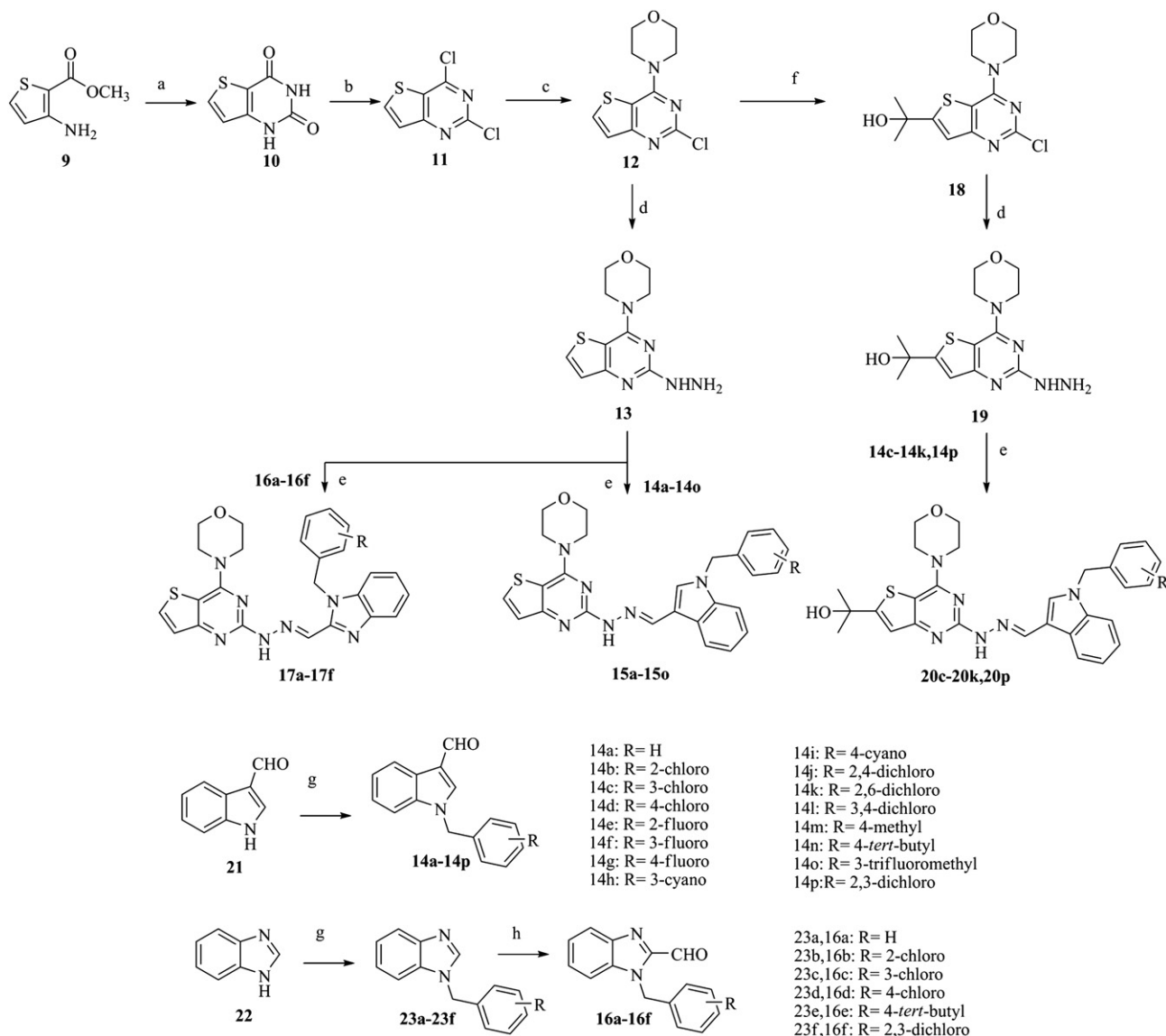


Fig. 2. Design strategy for 2-hydrazinyl-4-morpholinothieno[3,2-*d*]pyrimidine derivatives.



Scheme 1. Reagents and conditions: (a) 5eq urea, 190 °C, 2.5 h; (b) POCl₃, DMF(cat.), reflux, 8 h; (c) 2.1eq morpholine, MeOH, 0 °C, 30min, rt, 1–2 h; (d) 80% NH₂NH₂·H₂O, 80 °C, 4–6 h; (e) substituted aldehyde, reflux, 4–8 h; (f) acetone, *n*-BuLi, THF, –78 °C to rt, 5 h; (g) ArCH₂Cl, K₂CO₃, DMF, 80 °C; (h) DMF, *n*-BuLi, THF, –78 °C to rt, 6–8 h.

with the corresponding benzyl-1*H*-indole-3-carbaldehydes **14c–14k** and **14p** to afford the target compounds **20c–20k** and **20p**, respectively.

The substituted benzyl-1*H*-indole-3-carbaldehydes **14a–14p** were prepared by nucleophilic substitution of the various benzyl chloride with 1*H*-indole-3-carbaldehyde **21** in the presence of K₂CO₃ in *N,N*-dimethylformamide (DMF). The 1-benzyl-1*H*-benzo[d]imidazole-2-carbaldehydes **16a–16f** were synthesized via a two-step reaction. Reaction of benzimidazole with the corresponding benzyl chloride in the presence of K₂CO₃ in DMF yielded **23a–23f**. Subsequently, lithiation of **23a–23f**, followed by the addition of DMF, gave the aldehydes **16a–16f** in 75% yield.

The structures of target compounds were confirmed by IR, ¹H NMR, ¹³C NMR, 2D NOESY NMR and MS spectra. All the target compounds can exist in the *E* or *Z* isomeric forms due to the carbon–nitrogen double bonds formed in condensation reaction. The presence/absence of bulky groups and the differences in stability and energy are generally accepted as the main reasons for the preferential formation of one isomer over the other. It is interesting to note that the experimental procedure shown in

Scheme 1 led selectively to the *E* isomer, which was confirmed by 2D NOESY NMR spectroscopic approach with the aid of conformational analysis with Tripos Force Field by Sybyl 6.91 software package (TRIPOS Associates Inc.) (Figs. 3 and 4) [19,20].

For the representative compound **17a** or **20p**, the NOESY effect was observed between the proton of N–H and the proton in imine in *E* isomer (*E*-**17a** and *E*-**20p**) (see supplementary information), which should not be observed in the putative *Z* isomer (*Z*-**17a** and *Z*-**20p**) due to the larger intra-molecular H–H distances (Fig. 3). For compound **17a**, it is revealed experimentally by the NOESY spectrum, in which an evident cross-peak system from the dipolar interactions between N=CH (8.30, s) and N–H (11.43, s) is clear evidence of the presence of the *E*-**17a** isomer. Similarly, for compound **20p**, the NOE interactions between N=C–H (8.26, s) and N–H (10.48, s) confirmed the *E* isomer. Moreover, variable temperature experiments performed on *E*-**17a** and *E*-**20p** in the range 220–300 K do not produce any changes in the NMR spectra, revealing that *Z* and *E* isomers are not easily interconverted. On the basis of the above analysis, the relative stereochemistry of **17a** and **20p** was established unambiguously.

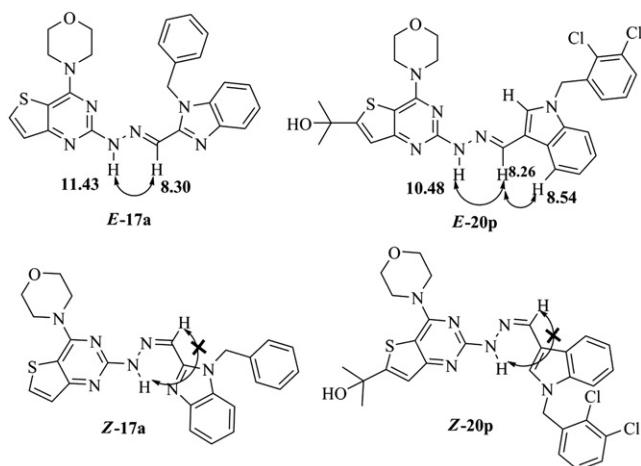


Fig. 3. Key NOESY of representative compounds **17a** and **20p**.

3. Results and discussion

3.1. Biological evaluation

The target compounds and their precursors **13**, **19** were evaluated for their cytotoxic activities against H460 (human lung cancer), HT-29 (human colon cancer), MDA-MB-231 (human breast cancer), U87MG (human glioblastoma) and H1975 (human lung cancer) cell lines *in vitro* together with reference compounds **4**, PAC-1 and GDC-0941 by MTT assay. In addition, the most promising compound **15f** was further evaluated against four cancer cell lines A549 (human lung cancer), H226 (human lung cancer), HepG2 (human liver cancer) and SGC-7901 (human stomach cancer). The results expressed as IC₅₀ were summarized in Tables 1 and 2 and the IC₅₀ values are the average of at least three independent experiments.

As illustrated in Table 1, most of the synthesized compounds showed moderate to significant cytotoxic activities and twenty-two of them were more potent than GDC-0941 against one or more cell lines. Nearly all the compounds were more active than their precursors **13**, **19**, suggesting that the presence of *N*-benzyl indole or *N*-benzyl benzimidazole hydrazinyl moiety enhanced their antitumor activities dramatically. The most promising compound **15f** showed strong cytotoxic activities against H460, HT-29 and MDA-MB-231 cell lines with IC₅₀ values of 0.23 μM, 0.39 μM and 1.11 μM, which were 3.8, 1.7 and 66.5 times more active than GDC-0941 (0.87 μM, 0.66 μM, 73.82 μM), respectively.

In general, the target compounds were more potent against H460 and HT-29 cell lines than against MDA-MB-231, U87MG and H1975 cell lines. These results suggested that this series of compounds possessed selectivity for H460 and HT-29 cancer cell lines. It's worth mentioning that almost all the target compounds

had higher potency than positive control GDC-0941 against MDA-MB-231 cancer cell line.

The SARs based on IC₅₀ values (Table 1) showed that variations in substitutions of the benzyl group had a marked impact on the cytotoxicity. For **15a–15o** and **20c–20k**, **20p**, substitution of the benzyl group at the 3-position or 4-position was well tolerated and 3-F substitution (**15f** and **20f**) produced the best potency. In most cases, compounds with substituents at the 3-position (**15c**, **15f**, **15h**, **20c**, **20f**, **20h**) were 2.6- to 12-folds more active than those without substituents at the same position (**15a**). Generally, electron-donating groups (EDGs) and weak electron-withdrawing groups (EWGs) at C-4 position were preferred. It was noticeable that strong EWGs at C-4 position weakened the activity dramatically, such as compounds **15i** and **20i** with cyano group at C-4 position were 1.9- to 38.7-folds weak relative to the positive control GDC-0941. Furthermore, small fluorine atom at 2-position of the benzyl group was more favorable, as compound **15e** was more potent than **15b** against all the tested cancer cell lines. However, introduction of two substituents (such as chlorine in this study) in the benzyl group resulted in a significantly decrease in activity, which might be due to its steric hindrance. It was obviously that compounds substituted by two chlorine groups (**15j–15l** and **20j–20l**) were more active than those with one chlorine group (**15b–15d** and **20c–20d**).

Further investigations were carried out in details to study the effect of hydroxy-isopropyl substituent at 6-position of the thienopyrimidine scaffold on the activity. It can be noted from Table 1 that the introduction of hydroxy-isopropyl group led to a remarkably increase in the activity against HT-29 and MDA-MB-231 cell lines and a slightly decrease against H460 cell line (**15c–15j** vs. **20c–20k**). This dramatic boost in the HT-29 and MDA-MB-231 potency and selectivity by the hydroxy-isopropyl substituent might be ascribed to the increased hydrogen bonds between the hydroxyl group and receptors necessary for activity.

Turning to the compounds **17a–17f**, interestingly, replacement of *N*-benzyl indole with its bioisostere *N*-benzyl benzimidazole moiety remarkably enhanced the activity and selectivity against HT-29 cancer cell line but failed to improve the activity against the other tested cell lines. In our opinion, these differences in pharmacological activity may be closely related to the electron densities of five-membered heterocycles and the specificity of cancer cells.

The cytotoxic activities of the most promising compound **15f** as well as GDC-0941 toward four additional cancer cell lines were shown in Table 2. Obviously, compound **15f** were more active than GDC-0941 against H226, SGC-7901 cell lines, which further confirmed its strong antitumor activity against different cancer lines.

3.2. 3D-QSAR study

3.2.1. 3D-QSAR model

All structures of thieno[3,2-*d*]pyrimidine derivatives were built and aligned onto the common substructure 2-hydrazinyl-4-

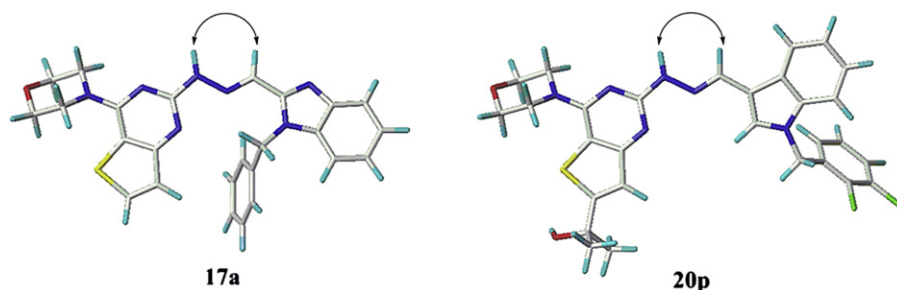
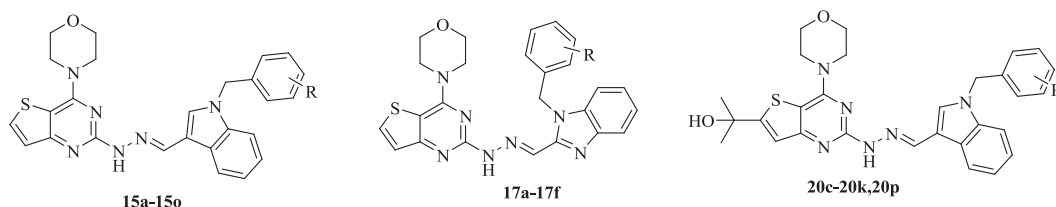


Fig. 4. Global optimal conformations for compounds **17a** (left) and **20p** (right) generated by Sybyl 6.91 software package.

Table 1
Structures and cytotoxic activities of compounds **13**, **19**, **15a–15o**, **17a–17f**, **20c–20k** and **20p** against H460, HT-29, MDA-MB-231, U87MG and H1975 cancer cell lines *in vitro*.



Compd.	R	IC ₅₀ (μM) ^a					pIC ₅₀ ^b
		H460	HT29	MDA-MB-231	U87MG	H1975	
13	–	42.21 ± 3.01	23.42 ± 3.13	63.75 ± 4.01	ND	ND	–
19	–	29.66 ± 2.58	56.21 ± 5.02	>100	ND	ND	–
15a	H	1.41 ± 0.13	4.70 ± 0.72	12.39 ± 1.49	>100	42.74 ± 2.24	5.85
15b	2-chloro	3.98 ± 0.11	>100	>100	ND	ND	5.40
15c	3-chloro	0.54 ± 0.09	2.98 ± 0.45	9.74 ± 1.41	5.96 ± 0.73	>100	6.27
15d	4-chloro	0.36 ± 0.085	5.76 ± 0.95	2.7 ± 0.56	15.64 ± 1.54	ND	6.45
15e	2-fluoro	0.86 ± 0.22	3.28 ± 0.48	9.24 ± 1.74	22.58 ± 0.59	>100	6.06
15f	3-fluoro	0.23 ± 0.095	0.39 ± 0.056	1.11 ± 0.061	12.59 ± 0.46	19.01 ± 0.78	6.65
15g	4-fluoro	0.41 ± 0.04	1.79 ± 0.12	12.32 ± 1.67	8.83 ± 1.03	>100	6.39
15h	3-cyano	0.34 ± 0.13	4.86 ± 1.14	2.0 ± 0.043	9.68 ± 0.21	ND	6.46
15i	4-cyano	1.62 ± 0.21	25.51 ± 2.21	>100	ND	ND	5.79
15j	2,4-dichloro	5.77 ± 0.33	46.52 ± 3.17	>100	ND	ND	5.24
15k	2,6-dichloro	10.42 ± 1.41	35.36 ± 3.07	20.47 ± 2.15	ND	ND	4.98
15l	3,4-dichloro	0.74 ± 0.21	16.20 ± 2.46	>100	>100	>100	6.13
15m	4-methyl	0.83 ± 0.14	3.31 ± 0.69	9.73 ± 2.08	4.97 ± 0.19	33.12 ± 1.69	6.08
15n	4-tert-butyl	0.38 ± 0.098	1.69 ± 0.35	1.43 ± 0.075	11.23 ± 0.63	8.00 ± 1.01	6.42
15o	3-trifluoromethyl	0.52 ± 0.070	1.68 ± 0.23	83.77 ± 5.01	4.84 ± 0.37	2.79 ± 0.52	6.28
17a	H	25.56 ± 1.41	1.08 ± 0.27	21.26 ± 1.87	ND	ND	4.59
17b	2-chloro	79.36 ± 3.52	0.40 ± 0.091	>100	ND	ND	4.10
17c	3-chloro	4.56 ± 0.12	1.01 ± 0.12	37.68 ± 3.21	ND	ND	5.34
17d	4-chloro	2.60 ± 0.31	0.77 ± 0.054	13.88 ± 0.64	13.37 ± 2.11	ND	5.58
17e	4-tert-butyl	3.62 ± 0.27	4.18 ± 1.39	8.17 ± 0.51	ND	ND	5.44
17f	2,3-dichloro	37.14 ± 4.21	6.46 ± 1.01	>100	ND	ND	4.43
20c	3-chloro	0.84 ± 0.069	0.87 ± 0.028	3.22 ± 0.42	8.91 ± 1.08	23.75 ± 0.25	6.08
20d	4-chloro	0.55 ± 0.095	0.87 ± 0.042	5.14 ± 0.76	7.43 ± 1.04	33.78 ± 1.32	6.26
20e	2-fluoro	1.10 ± 0.064	1.05 ± 0.127	1.66 ± 0.082	3.92 ± 0.86	15.56 ± 0.72	5.96
20f	3-fluoro	0.42 ± 0.07	0.38 ± 0.058	7.20 ± 0.36	7.82 ± 1.12	19.66 ± 0.32	6.37
20g	4-fluoro	1.10 ± 0.57	1.01 ± 0.097	1.53 ± 0.073	ND	ND	5.96
20h	3-cyano	0.36 ± 0.097	1.39 ± 0.089	5.61 ± 0.31	6.64 ± 0.87	ND	6.44
20i	4-cyano	4.53 ± 1.63	2.54 ± 0.147	6.31 ± 1.07	ND	ND	5.34
20j	2,4-dichloro	8.90 ± 0.81	5.38 ± 0.91	>100	ND	ND	5.05
20k	2,6-dichloro	4.03 ± 0.72	3.36 ± 0.65	62.12 ± 1.21	ND	ND	5.39
20p	2,3-dichloro	7.22 ± 1.21	3.70 ± 0.32	>100	ND	ND	5.14
4^c	–	9.2 ± 1.35	20.2 ± 2.09	>100	ND	ND	–
PAC-1^c	–	3.57 ± 1.62	0.97 ± 0.053	6.11 ± 0.75	ND	ND	–
GDC-0941^c	–	0.87 ± 0.20	0.66 ± 0.081	73.82 ± 3.06	7.77 ± 0.89	0.27 ± 0.021	–

Bold values show IC₅₀ of < 1 μM. ND: Not determined.

^a IC₅₀: concentration of the compound (μM) producing 50% cell growth inhibition after 72 h of drug exposure, as determined by the MTT assay. Each experiment was run at least three times.

^b pIC₅₀ values of H460 human tumor cell lines.

^c Used as a positive control.

morpholinothieno[3,2-*d*]pyrimidine nucleus (Fig. 5a, shown in bold), with the potent compound **15f** (Fig. 5a) as template. The structure alignment was illustrated in Fig. 5b. To further investigate the SARs of thieno[3,2-*d*]pyrimidine derivatives, the cytotoxic data

Table 2
Cytotoxic activities of compound **15f** and GDC-0941 against A549, H226, HepG2 and SGC-7901 cancer cell lines *in vitro*.

Compd.	IC ₅₀ (μM) ^a			
	A549	H226	HepG2	SGC-7901
15f	8.7 ± 0.92	0.91 ± 0.14	1.1 ± 0.21	0.8 ± 0.11
GDC-0941^b	6.9 ± 0.45	2.9 ± 0.64	1.0 ± 0.23	1.8 ± 0.69

^a IC₅₀: concentration of the compound (μM) producing 50% cell growth inhibition after 72 h of drug exposure, as determined by the MTT assay. Each experiment was run at least three times.

^b Used as a positive control.

of H460 cell line were used to build the 3D-QSAR models. 31 compounds with determinate IC₅₀ values were employed and their pIC₅₀ values were calculated based on the original IC₅₀ data. The detailed operation steps were similar to the methods in literature and were shown in the experimental section [21–23].

3.2.2. CoMFA and CoMSIA analysis

The PLS statistic results of CoMFA and CoMSIA models were summarized in Table 3. The predicted versus the experiment pIC₅₀ values are listed in Table 4 and are depicted graphically in Fig. 6 for CoMFA and CoMSIA models, respectively. The cross-validation correlation coefficient (q^2) which marked the predictive capacity and the conventional correlation coefficient (r^2) which marked self-consistence were two key parameters to evaluate the qualities of PLS analysis. A q^2 value over 0.3 is considered significant for the chance of significant correlation being <95%. For CoMFA model, the

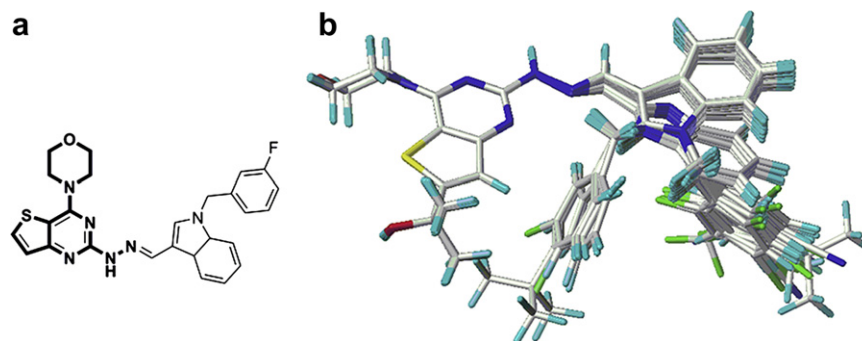


Fig. 5. (a) Structure of the template compound **15f**, common substructure is in bold, (b) 3D-QSAR structure alignment and superposition of 31 compounds using compound **15f** as the template.

q^2 and r^2 was 0.436 and 0.937, while for CoMSIA was 0.706 and 0.947. The statistic results indicated good predictive ability of CoMFA and CoMSIA models. The optimal numbers of components using to generate CoMFA and CoMSIA models is 6 and 5, respectively, which were reasonable according to the number of compounds used to derive the models. The standard errors of estimate of CoMFA and CoMSIA models were also reasonably low amounting to 0.186 and 0.167. Fisher test results were 59.326 and 89.399 for CoMFA and CoMSIA models, respectively. As shown in Table 3, for CoMFA model, the contributions of steric, electrostatic fields were 50.4% and 49.6%, while the contributions of steric, electrostatic, hydrophobic, hydrogen bond donor and acceptor fields of CoMSIA model were 8.9%, 30.8%, 44.8%, 2.1%, and 13.4%, respectively. The CoMFA and CoMSIA models established in the present study are quite reliable and sufficiently efficient in guiding further plausible modification in the molecules for obtaining better activity.

3.2.3. Contour analysis

To view the field effect on the target property, CoMFA and CoMSIA contour maps were generated. The contour maps can identify the important regions where any change in the steric, electrostatic, hydrophobic, hydrogen bond donor and hydrogen bond acceptor fields may affect the biological activity. The visualization of the results of the CoMFA and CoMSIA models were performed using the StDev*Coeff mapping option contoured by contribution. All of the contours represented the default 80 and 20% level contributions for favored and disfavored regions. 3D-QSAR contour maps of both CoMFA and CoMSIA models were depicted in Figs. 7 and 8, compounds **15f** with the highest pIC₅₀ value and **17d** were chosen to superimpose into the contour maps to better illustrate the SAR information.

3.2.3.1. CoMFA contour analysis. The CoMFA contour map of steric field is shown in Fig. 7(A). The green contours are indicative of

favorable regions for sterically bulkier groups and the yellow contours are indicative of regions that are sterically less favorable. There is one big green contour covering the 3- and 4-position of the benzyl group as shown in Fig. 7(A), which may explain why compounds **15a** (R = H) is less potent than compounds **15m** (R = 4-methyl), **15n** (4-*tert*-butyl) and **15o** (3-trifluoromethyl). Conversely, the sterically unfavorable regions indicated by yellow contours spotted around the 2- and 6-position of the benzyl group, as observed for the activity order of those compounds, **15e** (2-fluoro) > **15b** (2-chloro), **15j** (2,4-dichloro) > **15k** (2,6-dichloro), and **20e** (2-fluoro) > **20j** (2,4-dichloro), **20k** (2,6-dichloro), **20p** (2,3-dichloro).

The contour map of the electrostatic field of CoMFA model is shown in Fig. 7 (B). The red contours represent regions that lead to the enhancement of activity with electron rich groups, and contrary to that the blue regions represent electron deficient regions and can lead to an increase in the activity of compounds. Several small red regions are found around the 3-(5-) or 4-position of the benzyl group, which can explain the fact that compound **15i** (R = 4-cyano) is less active than compounds **15d** (2-chloro), **15g** (4-fluoro), **15m** (R = 4-methyl) and **15n** (4-*tert*-butyl), and compound **20i** (R = 4-cyano) is less active than compounds **20d** (2-chloro) and **20g** (4-fluoro). On the other hand, the blue contour near the 2-position and 6-position of benzene ring sheds light on the fact that the activity of compound **15e** (R = 2-fluoro) is higher than those of the compounds **15b** (R = 2-chloro), **15j** (R = 2, 4-dichloro) and **15k** (R = 2,6-dichloro).

3.2.3.2. CoMSIA contour analysis. The CoMSIA contour maps, derived from using steric, electrostatic, hydrophobic, hydrogen bond donor and hydrogen bond acceptor fields, are represented in Fig. 8. CoMSIA steric and electrostatic contours (Fig. 8(A) and (B)) are similar to those of CoMFA. However, some differences are noted as well. In case of CoMSIA, there is a large yellow contour overlapping the benzene ring, revealing that bulkier substituents will not be preferred in this region.

Table 3

PLS statistics of CoMFA and CoMSIA 3D-QSAR models.

	q^2 ^a	N^b	r^2 ^c	SE ^d	F^e	Fraction ^f				
						Steric	Electrostatic	Hydrophobic	Donor	Acceptor
CoMFA	0.436	6	0.937	0.186	59.326	0.504	0.496	–	–	–
CoMSIA	0.706	5	0.947	0.167	89.399	0.089	0.308	0.448	0.021	0.134

^a Cross-validated correlation coefficient.

^b Optimum number of components obtained from cross-validated PLS analysis and same used in final non-cross-validated analysis.

^c Non-cross-validated correlation coefficient.

^d Standard error of estimate.

^e F-test value.

^f Field contributions.

Table 4
Experimental and predicted activities against H460 cell line (pIC₅₀) of the target compounds for CoMFA and CoMSIA models.

Compd.	CoMFA			CoMSIA		
	pIC ₅₀ (experimental)	pIC ₅₀ (predicted)	Residuals	pIC ₅₀ (experimental)	pIC ₅₀ (predicted)	Residuals
15a	5.85	6.027	-0.1772	5.85	6.056	-0.2063
15b	5.40	5.813	-0.4126	5.40	5.709	-0.3091
15c	6.27	6.237	0.0329	6.27	6.291	-0.0210
15d	6.45	6.255	0.1955	6.45	6.264	0.1862
15e	6.06	5.961	0.0989	6.06	6.069	-0.0087
15f	6.65	6.369	0.2814	6.65	6.242	0.4078
15g	6.39	6.254	0.1360	6.39	6.23	0.1600
15h	6.46	6.323	0.1371	6.46	6.591	-0.1315
15i	5.79	5.939	-0.1487	5.79	5.580	0.2105
15j	5.24	5.163	0.0765	5.24	5.361	-0.1212
15k	4.98	4.916	0.0640	4.98	4.985	-0.0053
15l	6.13	6.237	-0.1075	6.13	6.154	-0.0242
15m	6.08	6.231	-0.1507	6.08	6.185	-0.1049
15n	6.42	6.449	-0.0291	6.42	6.366	0.0536
15o	6.28	6.28	0.0005	6.28	6.35	-0.0698
17a	4.59	5.033	-0.4430	4.59	4.942	-0.3524
17b	4.10	4.158	-0.0580	4.10	4.098	0.0022
17c	5.34	5.136	0.2043	5.34	5.251	0.0889
17d	5.58	5.367	0.2131	5.58	5.374	0.2061
17e	5.44	5.459	-0.0189	5.44	5.393	0.0466
17f	4.43	4.348	0.0819	4.43	4.427	0.0031
20c	6.08	6.146	-0.0659	6.08	6.205	-0.1254
20d	6.26	6.189	0.0707	6.26	6.318	-0.0577
20e	5.96	5.954	0.0059	5.96	5.952	0.0080
20f	6.37	6.486	-0.1162	6.37	6.464	-0.0945
20g	5.96	5.980	-0.0198	5.96	6.001	-0.0412
20h	6.44	6.392	0.0482	6.44	6.397	0.0433
20i	5.34	5.481	-0.1408	5.34	5.285	0.0550
20j	5.05	4.862	0.1882	5.05	4.960	0.0895
20k	5.39	5.267	0.1234	5.39	5.267	0.1226
20p	5.14	5.210	-0.0704	5.14	5.150	-0.0104

The hydrophobic contour map of CoMSIA model is displayed in Fig. 8(C). In the CoMSIA hydrophobic field, yellow regions and white regions indicate the areas where hydrophobic and hydrophilic properties are preferred, respectively. Two big yellow contours near the 3- and 4- positions of benzene ring (both of **15f** and **17d**) indicate the necessity of the hydrophobic group attached to the benzene ring for higher activity. This is a possible reason why compounds **15m** (R = 4-methyl) and **15o** (R = 4-*tert*-butyl) have higher potency than compound **15a** (R = H), and why compounds **17c** (R = 4-chloro), **17e** (R = 4-*tert*-butyl) are more active than **17a** (R = H). There is one white contour near the C-2 position of benzene ring, suggesting that hydrophilic groups in this region are beneficial to the activity.

The hydrogen bond donor contour map of CoMSIA model is displayed in Fig. 8(D). In the CoMSIA hydrogen bond donor field, hydrogen bond donor favored regions are represented by cyan contours and unfavorable regions by purple contours. The big cyan contour near -NH- functional group specifies that hydrogen bond donor is favored there. The little blue contour near thiophene ring is consistent with the fact that almost all the compounds with hydroxy-isopropyl groups (**15c–15i**) are less potent than those without substituents at the same position (**20c–20i**). This suggests that the hydroxy-isopropyl group at this position is not favorable for the cytotoxic activity against H460 cell line.

The hydrogen bond acceptor contour map of CoMSIA model is displayed in Fig. 8(E). In the CoMSIA hydrogen acceptor field, magenta contours represent regions where hydrogen bond acceptor substituents on ligands can be favored and the red ones represent areas where such substituents on compounds may be disfavored. It can be found that there is one big magenta region around the imino group, which proved the importance of thiopharmacophore for all the target compounds. The red region close

to the nitrogen atom of imidazole ring is in agreement with the fact that compounds containing benzimidazole moieties (**17a–17f**) are generally less potent than those with indole moieties (**15a–15o**, **20c–20k**, **20p**). Another red contour around 4-position of benzene ring could explain why compound **15i** with cyano group in this position is less potent than those without hydrogen bond acceptor group (**15d**, **15g**, **15m–15n**), and why **20i** (R = 4-cyano) is less potent than compounds **20d** (R = 4-chloro) and **20g** (R = 4-fluoro).

4. Conclusions

In summary, thirty-one thieno[3,2-*d*]pyrimidines bearing flexible substituted hydrazinyl groups at C2-position were designed and synthesized. Twenty-two of them were more potent than GDC-0941 and compound **15f** showed strongest cytotoxic activities against H460, HT-29 and MDA-MB-231 cell lines which were 3.8, 1.7 and 66.5 times more active than GDC-0941, respectively. The initial SARs showed that the flexible group benzyl-indole or benzyl-benzimidazole hydrazinyl moieties were necessary for these compounds to possess potent cytotoxic activities and the former were much better. Variations in substitutions of the benzyl group had a significant impact on the cytotoxicity. Substitution of the benzyl group at the 3-position or 4-position was well tolerated and 3-F substitution produced the best potency. Moreover, the introduction of hydroxy-isopropyl group was benefit to the selectivity for HT-29 cell line. Both CoMFA ($q^2 = 0.436$, $r^2 = 0.937$) and CoMSIA ($q^2 = 0.706$, $r^2 = 0.947$) models gave good statistical results in terms of q^2 and r^2 values, and provided significant insights that could be used in the further design of novel, potent and selective cytotoxic agents. Studies on the mechanism of action of these compounds are in progress and will be reported in the future.

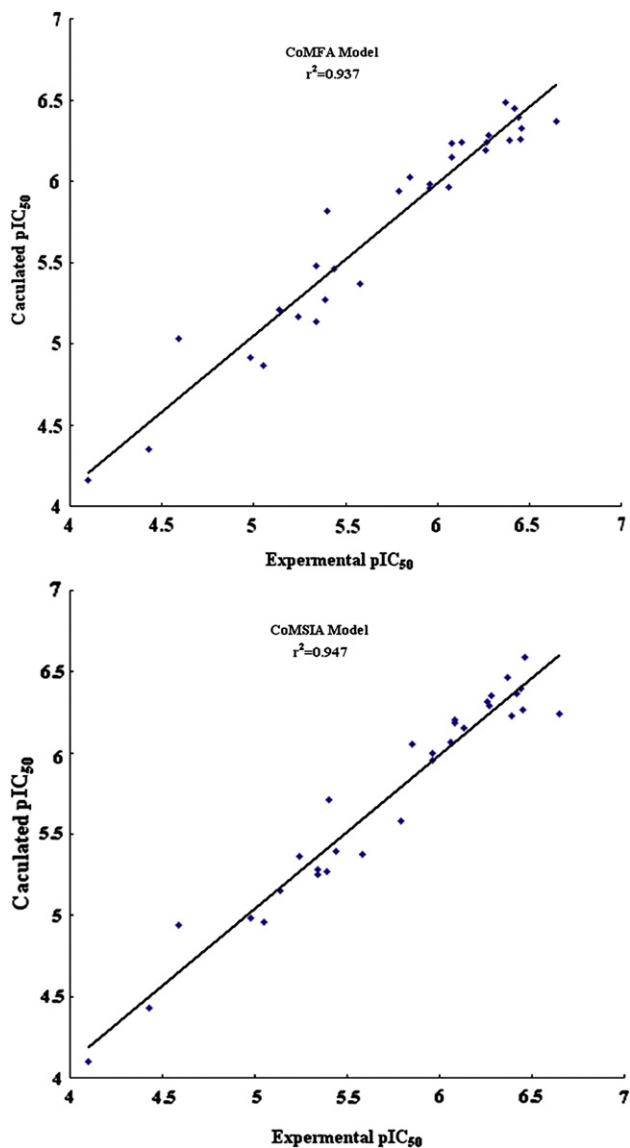


Fig. 6. Calculated pIC_{50} versus experimental pIC_{50} values for the 31 molecules obtained by PLS analysis using CoMFA and CoMSIA models.

5. Experimental

5.1. Chemistry

All melting points were obtained on a Büchi Melting Point B-540 apparatus (Büchi Labortechnik, Flawil, Switzerland) and were uncorrected. The IR spectra were recorded by means of the KBr pellet technique on a Bruker FTS 135 spectrometer. 1H NMR and ^{13}C NMR spectra were recorded on Bruker ARX-300, 300 MHz or Bruker ARX-600, 600 MHz spectrometers (Bruker Bioscience, Billerica, MA, USA) with TMS as an internal standard. Mass spectra (MS) were taken in ESI mode on Agilent 1100 LC–MS (Agilent, Palo Alto, CA, USA). Elemental analysis was determined on a Carlo-Erba 1106 Elemental analysis instrument (Carlo Erba, Milan, Italy). TLC analysis was carried out on silica gel plates GF254 (Qindao Haiyang Chemical, China). All the materials were obtained from commercial suppliers and used without purification, unless otherwise specified. Yields were not optimized.

5.2. Preparation of 1*H*-thieno[3,2-*d*]pyrimidine-2,4-dione (**10**)

A mixture of methyl 3-amino-2-thiophenecarboxylate (100 g, 0.64 mol) and urea (191 g, 3.2 mol) was heated at 190 °C for 2.5 h. Upon cooling to about 120 °C, the reaction mixture was poured into sodium hydroxide (2000 mL, 1N) solution and any insoluble material removed by filtration. The mixture was then acidified (HCl, 2N) to yield 1*H*-thieno[3,2-*d*]pyrimidine-2,4-dione as a white precipitate, which was collected by filtration and dried (105 g, 98%). m.p. >300 °C. ESI-MS m/z : 167.1 $[M - H]^-$. 1H NMR (300 MHz, DMSO- d_6) δ : 6.93 (d, $J = 5.2$ Hz, 1H), 8.04 (d, $J = 5.2$ Hz, 1H), 11.19 (s, 1H), 11.61 (s, 1H).

5.3. Preparation of 2, 4-dichloro-thieno[3,2-*d*]pyrimidine (**11**)

A mixture of 1*H*-thieno[3,2-*d*]pyrimidine-2,4-dione (105 g, 0.63 mol), phosphorous oxychloride (1000 mL) and catalytic amount DMF (2 mL) was heated at reflux for 8 h and the reaction was monitored by TLC. The reaction mixture was concentrated under reduced pressure and the residue was poured onto ice/water with vigorous stirring yielding a precipitate. The mixture was then filtered to yield 2,4-dichloro-thieno[3,2-*d*]pyrimidine as a white solid (93 g, 72%). m.p. 142–144 °C. ESI-MS m/z : 205.3 $[M + H]^+$.

5.4. Preparation of 2-chloro-4-morpholine-4-yl-thieno[3,2-*d*]pyrimidine (**12**)

To the mixture of 2,4-dichloro-thieno[3,2-*d*]pyrimidine (93 g, 0.45 mol) and MeOH (1500 mL), morpholine (81 mL, 2.1 eq) was

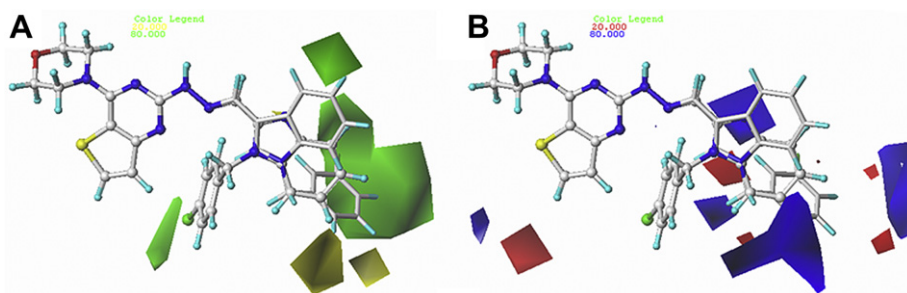


Fig. 7. CoMFA contour maps based on compounds **15f** (shown in capped sticks) and **17d** (shown in ball and stick). (A) CoMFA steric contours: green contours indicate regions where steric interaction is favored. Yellow contours are areas where the steric interaction is disfavored. (B) CoMFA electrostatic contours: the blue region represents the area where an electropositive group is favorable and the red region refers to the area where an electronegative group is favorable. (For interpretation of the references to color in this figure legend, the reader is referred to the web version of this article.)

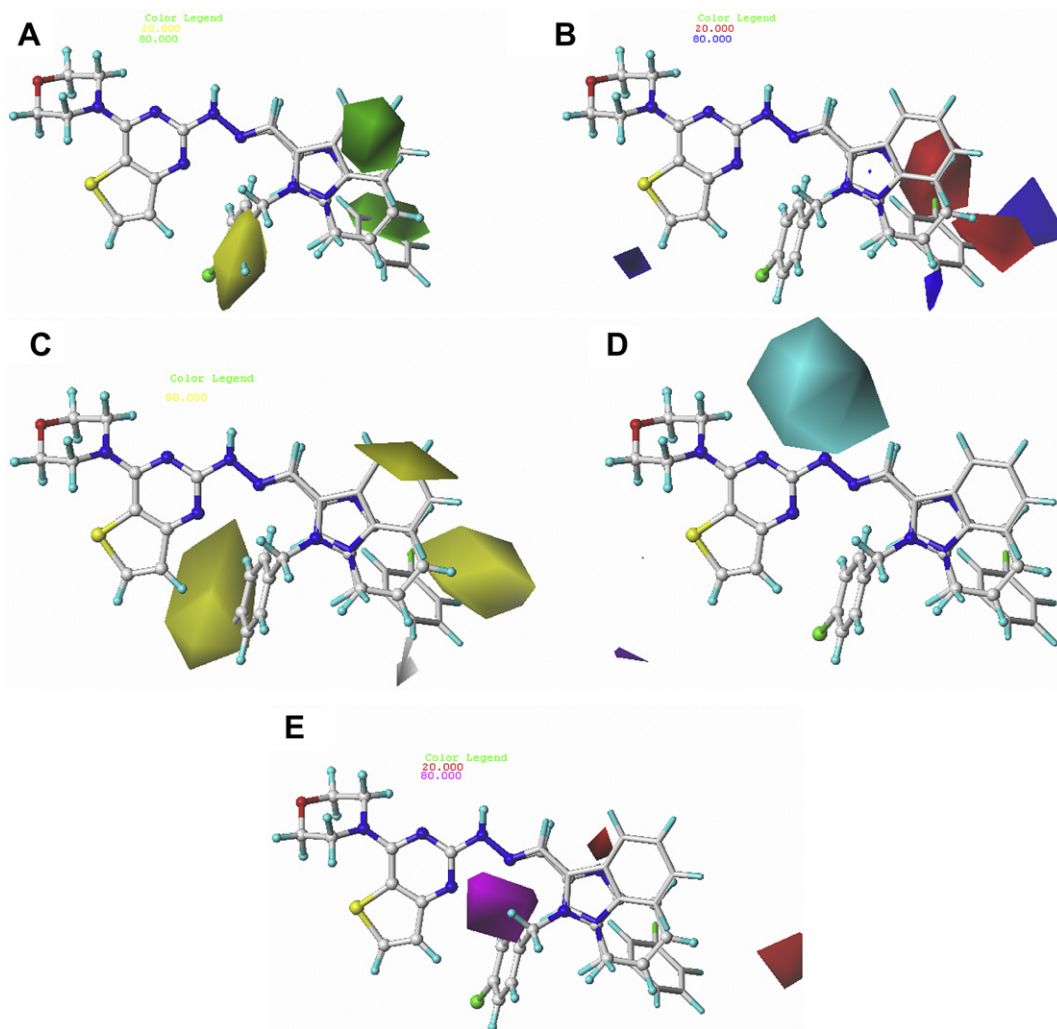


Fig. 8. CoMSIA contour maps based on compounds **15f** (shown in capped sticks) and **17d** (shown in ball & stick). (A) CoMSIA steric contour maps: green contour favours steric or bulky group and yellow contour denotes disfavored region. (B) CoMSIA electrostatic contour maps: blue contour indicates electropositive charge and red contour electronegative charge. (C) CoMSIA hydrophobic contour maps: yellow contours represent regions where hydrophobic groups increase activity, while white contours highlight regions that would favour hydrophilic groups. (D) CoMSIA hydrogen bond donor contours: cyan and purple contours represent favorable and unfavorable hydrogen bond donor regions, respectively. (E) CoMSIA hydrogen bond acceptor contours: magenta and red contours represent favorable and unfavorable hydrogen bond acceptor regions, respectively. (For interpretation of the references to color in this figure legend, the reader is referred to the web version of this article.)

added drop-wise at 0 °C. The reaction mixture then was stirred at room temperature for 1.5 h. After completion of reaction as indicated by TLC, the mixture was then filtered, washed with water and MeOH, to yield the title compound as a white solid (114 g, 98%). m.p. 204–205 °C. ESI-MS m/z : 255.9 [M + H]⁺, 277.6 [M + Na]⁺. ¹H NMR (300 MHz, DMSO-*d*₆) δ : 3.76 (s, 4H), 3.90 (d, J = 4.2 Hz, 4H), 7.41 (d, J = 5.4 Hz, 1H), 8.31 (d, J = 5.4 Hz, 1H).

5.5. Preparation of 4-(2-hydrazinylthieno[3,2-*d*]pyrimidin-4-yl)morpholine (**13**)

A solution of 80% hydrazine hydrate (NH₂NH₂·H₂O, 170 mL, 4.9 mol) and **12** (20.0 g, 0.078 mol) was stirred at 80 °C for 5 h. The precipitate was collected by filtration and washed with water, and dried to give **13** as a light yellow solid (13.4 g, 68%). m.p. 160–161 °C. ESI-MS m/z : 251.8 [M + H]⁺. ¹H NMR (600 MHz, DMSO-*d*₆) δ : 3.74–3.70 (m, 4H), 3.86–3.80 (m, 4H), 4.27 (s, 2H), 7.16 (d, J = 5.5 Hz, 1H), 7.54 (s, 1H), 8.00 (d, J = 5.5 Hz, 1H).

5.6. General procedure for the preparation of compounds **14a–14p**

1*H*-Indole-3-carbaldehyde **21** (14.5 g, 0.1 mol), together with the respective substituted benzyl chloride (0.11 mol) and anhydrous K₂CO₃ (27.6 g, 0.2 mol) were dissolved in *N,N*-dimethylformamide (30 mL) and heated at 80 °C for 5–8 h. Upon cooling to room temperature, the mixture was poured into ice-water and then the precipitated was collected by filtration and dried. The crude product was purified by recrystallized from ethanol to give the solids **14a–14p**.

5.7. General procedure for the preparation of compounds **16a–16f**

5.7.1. General procedure for the preparation of compounds **23a–23f**

1*H*-Benzo[*d*]imidazole **22** (11.8 g, 0.1 mol), together with the respective substituted benzyl chloride (0.11 mol) and anhydrous K₂CO₃ (27.6 g, 0.2 mol) were dissolved in DMF (30 mL) and heated at 50 °C for 5–6 h. Upon cooling to room temperature, the mixture was poured into ice-water and then the precipitated was collected

by filtration and dried. The crude product was purified by recrystallized from ethanol to give the solids **23a–23f**.

5.7.2. General procedure for the preparation of compounds **16a–16f**

To a stirred, cooled ($-78\text{ }^{\circ}\text{C}$) solution of substituted 1-benzyl-1*H*-benzo[d]imidazole **23a–23f** (0.03 mol) in 60 mL THF under nitrogen atmosphere was added dropwise *n*-butyllithium solution (0.04 mol, 2.5 M in hexanes) for half an hour. When addition was complete, stirring at $-75\text{ }^{\circ}\text{C}$ was continued for 1 h. The reaction mixture was then treated with 0.1 mol dried DMF within 10 min and stirring at $-75\text{ }^{\circ}\text{C}$ for 1 h. The mixture was then allowed to warm to ambient temperature and stirred for a future 2 h. The reaction was quenched with saturated NH_4Cl (50 mL) and extracted with ether (100 mL \times 2). The organic phase was washed with brine, dried (MgSO_4), filtered and concentrated. The crude product was purified by chromatography on silica gel using petroleum/EtOAc to give substituted 1-benzyl-1*H*-benzo[d]imidazole-2-carbaldehyde **16a–16f**.

5.8. General procedure for preparation of compounds **15a–15o** and **17a–17f**

A mixture of 4-(2-hydrazinylthieno[3,2-*d*]pyrimidin-4-yl)morpholine **13** (0.12 g, 0.48 mmol), substituted benzyl-1*H*-indole-3-carbaldehyde **14a–14o** or 1-benzyl-1*H*-benzo[d]imidazole-2-carbaldehyde **16a–16f** (0.48 mmol) and a drop of glacial acetic acid in absolute ethanol (8 mL) was refluxed for 4–8 h. The mixture was cooled, separated by filtration and washed with EtOH to give off a white to light yellow solid. The crude product was recrystallized from ethanol or purified by chromatography on silica gel using $\text{MeOH}/\text{CH}_2\text{Cl}_2$ to afford the solids **15a–15o** and **17a–17f**.

5.8.1. (*E*)-4-(2-(2-((1-benzyl-1*H*-indol-3-yl)methylene)hydrazinyl)thieno[3,2-*d*]pyrimidin-4-yl)morpholine (**15a**)

This compound was obtained as off-white solid in 85% yield. m.p. $256\text{--}258\text{ }^{\circ}\text{C}$. ESI-MS m/z : 469.1 $[\text{M} + \text{H}]^+$. IR (KBr) cm^{-1} : 3437.2, 3171.5, 2964.6, 2854.3, 1537.0, 1364.4, 1343.8, 1008.9, 786.6, 744.5, 727.9. ^1H NMR (300 MHz, $\text{DMSO-}d_6$) δ : 3.80 (d, $J = 4.7$ Hz, 4H), 3.97 (d, $J = 4.5$ Hz, 4H), 5.43 (s, 2H), 7.37–7.07 (m, 8H), 7.48 (d, $J = 7.8$ Hz, 1H), 7.81 (s, 1H), 8.04 (t, $J = 6.7$ Hz, 1H), 8.28 (s, 1H), 8.49 (d, $J = 7.6$ Hz, 1H), 10.51 (s, 1H). Anal. Calcd for $\text{C}_{26}\text{H}_{24}\text{N}_6\text{O}$ (%): C, 66.64; H, 5.16; N, 17.94. Found (%): C, 66.56; H, 5.18; N, 17.98.

5.8.2. (*E*)-4-(2-(2-((1-(2-Chlorobenzyl)-1*H*-indol-3-yl)methylene)hydrazinyl)thieno[3,2-*d*]pyrimidin-4-yl)morpholine (**15b**)

This compound was obtained as light yellow powder in 87% yield. m.p. $247\text{--}249\text{ }^{\circ}\text{C}$. ESI-MS m/z : 503.1 (Cl = 35), 505.1 (Cl = 37) $[\text{M} + \text{H}]^+$. IR (KBr) cm^{-1} : 3435.6, 3253.6, 1539.2, 1372.8, 1274.2, 1172.7, 1120.2, 1013.7, 885.7, 789.7, 734.4. ^1H NMR (300 MHz, $\text{DMSO-}d_6$) δ : 3.81 (d, $J = 4.3$ Hz, 4H), 3.98 (s, 4H), 5.53 (s, 2H), 6.78 (d, $J = 7.5$ Hz, 1H), 7.38–7.12 (m, 5H), 7.41 (d, $J = 8.1$ Hz, 1H), 7.52 (d, $J = 7.8$ Hz, 1H), 7.74 (s, 1H), 8.06 (d, $J = 5.5$ Hz, 1H), 8.33 (s, 1H), 8.53 (d, $J = 7.1$ Hz, 1H), 10.58 (s, 1H). Anal. Calcd for $\text{C}_{26}\text{H}_{23}\text{ClN}_6\text{O}$ (%): C, 62.08; H, 4.61; N, 16.71. Found (%): C, 62.04; H, 4.63; N, 16.65.

5.8.3. (*E*)-4-(2-(2-((1-(3-Chlorobenzyl)-1*H*-indol-3-yl)methylene)hydrazinyl)thieno[3,2-*d*]pyrimidin-4-yl)morpholine (**15c**)

This compound was obtained as off-white solid in 86% yield. m.p. $238\text{--}240\text{ }^{\circ}\text{C}$. ESI-MS m/z : 503.1 (Cl = 35), 505.1 (Cl = 37) $[\text{M} + \text{H}]^+$. IR (KBr) cm^{-1} : 3442.3, 3173.5, 2852.7, 1536.9, 1432.7, 1366.3, 1339.7, 1166.0, 1120.3, 785.1, 746.9. ^1H NMR (300 MHz, $\text{DMSO-}d_6$) δ : 3.81 (d, $J = 4.4$ Hz, 4H), 3.98 (s, 4H), 5.45 (s, 2H), 7.27–7.06 (m, 4H), 7.34 (dd, $J_1 = 12.2$ Hz, $J_2 = 6.1$ Hz, 3H), 7.49 (d, $J = 7.9$ Hz, 1H), 7.84 (s, 1H), 8.05 (d, $J = 5.5$ Hz, 1H), 8.28 (s, 1H), 8.50 (d, $J = 7.3$ Hz, 1H), 10.53 (s, 1H). ^{13}C NMR ($\text{DMSO-}d_6$) δ : 164.31,

159.00, 158.76, 141.15, 137.43, 136.99, 133.96, 133.86, 131.39, 131.28, 128.21, 127.65, 126.53, 125.96, 124.47, 123.46, 123.35, 121.09, 113.56, 111.06, 106.27, 66.77 (2C), 49.25, 46.58 (2C). Anal. Calcd for $\text{C}_{26}\text{H}_{23}\text{ClN}_6\text{O}$ (%): C, 62.08; H, 4.61; N, 16.71. Found (%): C, 62.02; H, 4.63; N, 16.78.

5.8.4. (*E*)-4-(2-(2-((1-(4-Chlorobenzyl)-1*H*-indol-3-yl)methylene)hydrazinyl)thieno[3,2-*d*]pyrimidin-4-yl)morpholine (**15d**)

This compound was obtained as light yellow solid in 87% yield. m.p. $221\text{--}223\text{ }^{\circ}\text{C}$. ESI-MS m/z : 503.3 (Cl = 35), 505.3 (Cl = 37) $[\text{M} + \text{H}]^+$. IR (KBr) cm^{-1} : 3436.7, 2845.7, 1574.0, 1535.5, 1374.3, 1164.9, 1120.0, 1013.8, 745.5. ^1H NMR (300 MHz, $\text{DMSO-}d_6$) δ : 3.80 (s, 4H), 3.97 (s, 4H), 5.44 (s, 2H), 7.19 (m, 5H), 7.38 (d, $J = 8.2$ Hz, 2H), 7.47 (d, $J = 7.7$ Hz, 1H), 7.81 (s, 1H), 8.06 (d, $J = 5.5$ Hz, 1H), 8.27 (s, 1H), 8.48 (d, $J = 7.5$ Hz, 1H), 10.51 (s, 1H). ^{13}C NMR ($\text{DMSO-}d_6$) δ : 163.84, 158.90, 158.48, 137.47, 137.34, 133.94, 132.87, 131.41, 129.71(2C), 129.30 (2C), 128.90, 125.93, 124.31, 123.49, 123.19, 121.13, 113.28, 111.05, 106.43, 66.73 (2C), 49.25, 46.55 (2C). Anal. Calcd for $\text{C}_{26}\text{H}_{23}\text{ClN}_6\text{O}$ (%): C, 62.08; H, 4.61; N, 16.71. Found (%): C, 62.02; H, 4.58; N, 16.79.

5.8.5. (*E*)-4-(2-(2-((1-(2-Fluorobenzyl)-1*H*-indol-3-yl)methylene)hydrazinyl)thieno[3,2-*d*]pyrimidin-4-yl)morpholine (**15e**)

This compound was obtained as light yellow solid in 80% yield. m.p. $134\text{--}135\text{ }^{\circ}\text{C}$. ESI-MS m/z : 487.1 $[\text{M} + \text{H}]^+$. IR (KBr) cm^{-1} : 3428.8, 3051.1, 2856.3, 1539.6, 1380.4, 1168.4, 1115.0, 1016.1, 888.0, 753.6. ^1H NMR (300 MHz, $\text{DMSO-}d_6$) δ : 3.81 (d, $J = 4.7$ Hz, 4H), 3.94 (d, $J = 4.5$ Hz, 4H), 5.50 (s, 2H), 7.32–6.87 (m, 6H), 7.41–7.27 (m, 1H), 7.50 (d, $J = 8.0$ Hz, 1H), 7.75 (s, 1H), 8.05 (d, $J = 5.5$ Hz, 1H), 8.27 (s, 1H), 8.49 (d, $J = 7.4$ Hz, 1H), 10.51 (s, 1H). Anal. Calcd for $\text{C}_{26}\text{H}_{23}\text{FN}_6\text{O}$ (%): C, 64.18; H, 4.76; N, 17.27. Found (%): C, 64.14; H, 4.74; N, 17.29.

5.8.6. (*E*)-4-(2-(2-((1-(3-Fluorobenzyl)-1*H*-indol-3-yl)methylene)hydrazinyl)thieno[3,2-*d*]pyrimidin-4-yl)morpholine (**15f**)

This compound was obtained as off-white solid in 82% yield. m.p. $248\text{--}250\text{ }^{\circ}\text{C}$. ESI-MS m/z : 486.6 $[\text{M} + \text{H}]^+$. IR (KBr) cm^{-1} : 3436.4, 3174.1, 2965.1, 2853.7, 1537.0, 1489.5, 1365.8, 1342.3, 1248.9, 1166.5, 1119.8, 785.0, 744.1. ^1H NMR (300 MHz, $\text{DMSO-}d_6$) δ : 3.80 (s, 4H), 3.97 (s, 4H), 5.45 (s, 2H), 7.30–6.91 (m, 6H), 7.35 (d, $J = 7.2$ Hz, 1H), 7.49 (d, $J = 8.0$ Hz, 1H), 7.84 (s, 1H), 8.06 (d, $J = 5.4$ Hz, 1H), 8.28 (s, 1H), 8.49 (d, $J = 7.3$ Hz, 1H), 10.55 (s, 1H). Anal. Calcd for $\text{C}_{26}\text{H}_{23}\text{FN}_6\text{O}$ (%): C, 64.18; H, 4.76; N, 17.27. Found (%): C, 64.11; H, 4.77; N, 17.32.

5.8.7. (*E*)-4-(2-(2-((1-(4-Fluorobenzyl)-1*H*-indol-3-yl)methylene)hydrazinyl)thieno[3,2-*d*]pyrimidin-4-yl)morpholine (**15g**)

This compound was obtained as light yellow solid in 79% yield. m.p. $134\text{--}136\text{ }^{\circ}\text{C}$. ESI-MS m/z : 487.1 $[\text{M} + \text{H}]^+$. IR (KBr) cm^{-1} : 3433.5, 3070.9, 2925.6, 2857.1, 1616.1, 1559.9, 1381.8, 1282.1, 1252.6, 1177.0, 1115.9, 1016.8, 888.3, 780.4, 743.6. ^1H NMR (300 MHz, $\text{DMSO-}d_6$) δ : 3.80(d, $J = 4.6$ Hz, 4H), 3.96 (d, $J = 4.7$ Hz, 4H), 5.42 (s, 2H), 7.17 (t, $J_1 = 15.1$ Hz, $J_2 = 7.1$ Hz, 5H), 7.31 (dd, $J_1 = 8.5$ Hz, $J_2 = 5.6$ Hz, 2H), 7.49 (d, $J = 7.9$ Hz, 1H), 7.81 (s, 1H), 8.05 (d, $J = 5.5$ Hz, 1H), 8.27 (s, 1H), 8.48 (d, $J = 7.5$ Hz, 1H), 10.49 (s, 1H). Anal. Calcd for $\text{C}_{26}\text{H}_{23}\text{FN}_6\text{O}$ (%): C, 64.18; H, 4.76; N, 17.27. Found (%): C, 64.13; H, 4.74; N, 17.32.

5.8.8. (*E*)-3-((3-((2-(4-Morpholinthieno[3,2-*d*]pyrimidin-2-yl)hydrazono)methyl)-1*H*-indol-1-yl)methyl)benzotrile (**15h**)

This compound was obtained as pale yellow powder in 83% yield. m.p. $227\text{--}229\text{ }^{\circ}\text{C}$. ESI-MS m/z : 494.1 $[\text{M} + \text{H}]^+$. IR (KBr) cm^{-1} : 3443.6, 2854.5, 1539.3, 1372.5, 1172.4, 1118.3, 1016.2, 886.1, 789.5, 737.3. ^1H NMR (300 MHz, $\text{DMSO-}d_6$) δ : 3.81 (s, 4H), 3.98 (s, 4H), 5.50 (s, 2H), 7.31–7.01 (m, 3H), 7.62–7.42 (m, 3H), 7.82–7.65 (m, 2H), 7.86

(s, 1H), 8.05 (d, $J = 5.5$ Hz, 1H), 8.28 (s, 1H), 8.50 (d, $J = 7.5$ Hz, 1H), 10.53 (s, 1H). Anal. Calcd for $C_{27}H_{23}N_7OS$ (%): C, 65.70; H, 4.70; N, 19.86. Found (%): C, 65.66; H, 4.69; N, 19.92.

5.8.9. (*E*)-4-((3-((2-(4-Morpholinothieno[3,2-*d*]pyrimidin-2-yl)hydrazono)methyl)-1*H*-indol-1-yl)methyl)benzotrile (**15i**)

This compound was obtained as light yellow solid in 80% yield. m.p. 248–250 °C. ESI-MS m/z : 494.1 $[M + H]^+$. IR (KBr) cm^{-1} : 3436.3, 3242.3, 2951.7, 1614.0, 1538.3, 1510.6, 1352.8, 1170.6, 1014.0, 883.8, 789.6, 735.1. 1H NMR (300 MHz, DMSO- d_6) δ : 3.81 (s, 4H), 3.98 (s, 4H), 5.72 (s, 2H), 6.96 (d, $J = 7.7$ Hz, 1H), 7.35–7.09 (m, 3H), 7.47 (dd, $J_1 = 12.2$ Hz, $J_2 = 7.5$ Hz, 2H), 7.61 (t, $J = 7.4$ Hz, 1H), 7.77 (s, 1H), 7.91 (d, $J = 7.3$ Hz, 1H), 8.06 (d, $J = 5.5$ Hz, 1H), 8.28 (s, 1H), 8.53 (d, $J = 7.1$ Hz, 1H), 10.54 (s, 1H). Anal. Calcd for $C_{27}H_{23}N_7OS$ (%): C, 65.70; H, 4.70; N, 19.86. Found (%): C, 65.62; H, 4.68; N, 19.93.

5.8.10. (*E*)-4-(2-(2-((1-(2,4-Dichlorobenzyl)-1*H*-indol-3-yl)methylene)hydrazinyl)thieno[3,2-*d*]pyrimidin-4-yl)morpholine (**15j**)

This compound was obtained as light yellow solid in 88% yield. m.p. 138–140 °C. ESI-MS m/z : 537.1 (Cl = 35), 538.9 (Cl = 37) $[M + H]^+$. IR (KBr) cm^{-1} : 3436.6, 3069.8, 2856.8, 1559.7, 1382.7, 1252.6, 1177.8, 1115.3, 1016.5, 782.1, 742.8. 1H NMR (300 MHz, DMSO- d_6) δ : 3.81 (d, $J = 4.6$ Hz, 4H), 3.97 (d, $J = 4.4$ Hz, 4H), 5.55 (s, 2H), 6.75 (d, $J = 8.4$ Hz, 1H), 7.27–7.09 (m, 3H), 7.34 (dd, $J_1 = 8.4$ Hz, $J_2 = 2.1$ Hz, 1H), 7.41 (d, $J = 7.3$ Hz, 1H), 7.81–7.63 (m, 2H), 8.06 (d, $J = 5.5$ Hz, 1H), 8.27 (s, 1H), 8.53 (d, $J = 7.1$ Hz, 1H), 10.54 (s, 1H). Anal. Calcd for $C_{26}H_{22}Cl_2N_6OS$ (%): C, 58.10; H, 4.13; N, 15.64. Found (%): C, 58.04; H, 4.12; N, 15.70.

5.8.11. (*E*)-4-(2-(2-((1-(2,6-Dichlorobenzyl)-1*H*-indol-3-yl)methylene)hydrazinyl)thieno[3,2-*d*]pyrimidin-4-yl)morpholine (**15k**)

This compound was obtained as pale yellow solid in 89% yield. m.p. 239–241 °C. ESI-MS m/z : 537.4 (Cl = 35), 539.3 (Cl = 37) $[M + H]^+$. IR (KBr) cm^{-1} : 3428.4, 2854.2, 1539.7, 1371.6, 1171.8, 787.8, 741.7. 1H NMR (300 MHz, DMSO- d_6) δ : 3.80 (d, $J = 4.4$ Hz, 4H), 3.96 (d, $J = 4.2$ Hz, 4H), 5.57 (s, 2H), 7.17 (dd, $J_1 = 11.7$ Hz, $J_2 = 6.3$ Hz, 2H), 7.25 (d, $J = 11.2$ Hz, 2H), 7.54–7.41 (m, 1H), 7.60 (d, $J = 7.7$ Hz, 3H), 8.04 (d, $J = 5.5$ Hz, 1H), 8.18 (s, 1H), 8.49 (d, $J = 7.7$ Hz, 1H), 10.48 (s, 1H). Anal. Calcd for $C_{26}H_{22}Cl_2N_6OS$ (%): C, 58.10; H, 4.13; N, 15.64. Found (%): C, 58.05; H, 4.16; N, 15.67.

5.8.12. (*E*)-4-(2-(2-((1-(3,4-Dichlorobenzyl)-1*H*-indol-3-yl)methylene)hydrazinyl)thieno[3,2-*d*]pyrimidin-4-yl)morpholine (**15l**)

This compound was obtained as light yellow solid in 84% yield. m.p. 208–210 °C. ESI-MS m/z : 537.0 (Cl = 35), 539.1 (Cl = 37) $[M + H]^+$. IR (KBr) cm^{-1} : 3436.4, 2951.2, 1534.2, 1374.4, 1166.4, 1118.1, 1014.0, 747.3. 1H NMR (300 MHz, DMSO- d_6) δ : 3.81 (s, 4H), 3.98 (s, 4H), 5.46 (s, 2H), 7.34–7.10 (m, 4H), 7.50 (d, $J = 7.9$ Hz, 1H), 7.66–7.54 (m, 2H), 7.85 (s, 1H), 8.06 (d, $J = 5.5$ Hz, 1H), 8.28 (s, 1H), 8.49 (d, $J = 7.4$ Hz, 1H), 10.54 (s, 1H). Anal. Calcd for $C_{26}H_{22}Cl_2N_6OS$ (%): C, 58.10; H, 4.13; N, 15.64. Found (%): C, 58.02; H, 4.11; N, 15.73.

5.8.13. (*E*)-4-(2-(2-((1-(4-Methylbenzyl)-1*H*-indol-3-yl)methylene)hydrazinyl)thieno[3,2-*d*]pyrimidin-4-yl)morpholine (**15m**)

This compound was obtained as light yellow solid in 82% yield. m.p. 224–226 °C. ESI-MS m/z : 483.1 $[M + H]^+$. IR (KBr) cm^{-1} : 3436.5, 3048.7, 2922.5, 2857.9, 1561.3, 1382.4, 1252.2, 1176.5, 1115.1, 1017.2, 888.5, 780.5, 737.4. 1H NMR (300 MHz, DMSO- d_6) δ : 2.24 (s, 3H), 3.80 (d, $J = 4.6$ Hz, 4H), 3.96 (d, $J = 4.4$ Hz, 4H), 5.37 (s, 2H), 5.76 (s, 1H), 7.22–6.97 (m, 6H), 7.46 (d, $J = 7.9$ Hz, 1H), 7.78 (s, 1H), 8.05 (d, $J = 5.5$ Hz, 1H), 8.27 (s, 1H), 8.47 (d, $J = 7.5$ Hz, 1H), 10.50 (s, 1H). ^{13}C NMR (DMSO- d_6) δ : 164.30, 158.99, 158.75, 137.45, 137.17, 135.48, 133.83, 131.40, 129.86 (2C), 127.93 (2C), 125.97, 124.46, 123.24, 120.90, 113.21, 111.16, 106.25, 66.77 (2C), 55.66, 49.77, 46.57 (2C),

21.39. Anal. Calcd for $C_{27}H_{26}N_6OS$ (%): C, 67.20; H, 5.43; N, 17.41. Found (%): C, 67.05; H, 5.42; N, 17.49.

5.8.14. (*E*)-4-(2-(2-((1-(4-*tert*-butylbenzyl)-1*H*-indol-3-yl)methylene)hydrazinyl)thieno[3,2-*d*]pyrimidin-4-yl)morpholine (**15n**)

This compound was obtained as light yellow solid in 71% yield. m.p. 143–145 °C. ESI-MS m/z : 525.2 $[M + H]^+$. IR (KBr) cm^{-1} : 3428.9, 2960.6, 1652.9, 1540.7, 1378.3, 1248.9, 1170.9, 1014.9, 744.2. 1H NMR (300 MHz, DMSO- d_6) δ : 1.22 (s, 9H), 3.81 (s, 4H), 4.00 (s, 4H), 5.41 (s, 2H), 7.28–7.03 (m, 5H), 7.32 (d, $J = 8.1$ Hz, 2H), 7.50 (d, $J = 8.0$ Hz, 1H), 7.80 (s, 1H), 8.09 (d, $J = 5.4$ Hz, 1H), 8.31 (s, 1H), 8.48 (d, $J = 7.8$ Hz, 1H), 10.50 (s, 1H). ^{13}C NMR (DMSO- d_6) δ : 164.46, 164.28, 158.98, 158.74, 150.62, 137.49, 137.17, 135.58, 133.84, 131.40, 127.65 (2C), 126.07 (2C), 125.93, 124.46, 123.27, 120.90, 113.25, 111.14, 106.29, 66.76 (2C), 49.60, 46.57 (2C), 34.93, 31.80 (3C). Anal. Calcd for $C_{30}H_{32}N_6OS$ (%): C, 68.67; H, 6.15; N, 16.02. Found (%): C, 68.59; H, 6.12; N, 16.09.

5.8.15. (*E*)-4-(2-(2-((1-(3-(Trifluoromethyl)benzyl)-1*H*-indol-3-yl)methylene)hydrazinyl)thieno[3,2-*d*]pyrimidin-4-yl)morpholine (**15o**)

This compound was obtained as light yellow solid in 78% yield. m.p. 136–137 °C. ESI-MS m/z : 537.2 $[M + H]^+$. IR (KBr) cm^{-1} : 3435.8, 3071.1, 1619.1, 1560.1, 1384.0, 1334.3, 1110.9, 1075.4, 888.8, 781.0, 742.6, 700.8. 1H NMR (300 MHz, DMSO- d_6) δ : 3.80 (s, 4H), 3.98 (s, 4H), 5.56 (s, 2H), 7.35–7.02 (m, 3H), 7.79–7.38 (m, 5H), 7.92 (s, 1H), 8.07 (d, $J = 5.4$ Hz, 1H), 8.29 (s, 1H), 8.50 (d, $J = 7.3$ Hz, 1H), 10.59 (s, 1H). ^{13}C NMR (DMSO- d_6) δ : 172.79, 158.94, 158.48, 140.10, 137.45, 137.28, 134.00, 131.90, 131.50, 130.51, 125.95, 125.05, 125.0, 124.42, 124.29, 123.52, 123.38, 121.15, 113.58, 111.02, 106.36, 66.76 (2C), 49.30, 46.60 (2C), 21.80. Anal. Calcd for $C_{27}H_{23}F_3N_6OS$ (%): C, 60.21; H, 4.68; N, 15.66. Found (%): C, 60.07; H, 4.66; N, 15.79.

5.8.16. (*E*)-4-(2-(2-((1-benzyl)-1*H*-benzo[*d*]imidazol-2-yl)methylene)hydrazinyl)thieno[3,2-*d*]pyrimidin-4-yl)morpholine (**17a**)

This compound was obtained as pale yellow solid in 68% yield. m.p. 268–270 °C. ESI-MS m/z : 470.3 $[M + H]^+$. IR (KBr) cm^{-1} : 3432.6, 3245.7, 1572.9, 1539.4, 1353.4, 1276.8, 1177.5, 888.8, 740.3. 1H NMR (300 MHz, DMSO- d_6) δ : 3.56 (s, 4H), 3.73 (s, 4H), 6.20 (s, 2H), 7.25 (dt, $J_1 = 12.0$ Hz, $J_2 = 6.6$ Hz, 6H), 7.38 (d, $J = 7.0$ Hz, 2H), 7.48 (d, $J = 5.7$ Hz, 1H), 7.79–7.58 (m, 1H), 8.12 (d, $J = 5.5$ Hz, 1H), 8.30 (s, 1H), 11.43 (s, 1H). Anal. Calcd for $C_{25}H_{23}N_7OS$ (%): C, 63.95; H, 4.94; N, 20.88. Found (%): C, 63.86; H, 4.92; N, 20.94.

5.8.17. (*E*)-4-(2-(2-((1-(2-Chlorobenzyl)-1*H*-benzo[*d*]imidazol-2-yl)methylene)hydrazinyl)thieno[3,2-*d*]pyrimidin-4-yl)morpholine (**17b**)

This compound was obtained as pale yellow solid in 71% yield. m.p. 281–283 °C. ESI-MS m/z : 504.2 $[M + H]^+$, 526.2 $[M + Na]^+$. IR (KBr) cm^{-1} : 3425.4, 2963.6, 2854.4, 1571.3, 1538.0, 1443.0, 1361.6, 1177.7, 788.0, 750.3. 1H NMR (300 MHz, DMSO- d_6) δ : 3.61 (d, $J = 4.4$ Hz, 4H), 3.71 (d, $J = 4.3$ Hz, 4H), 6.29 (s, 2H), 6.62 (d, $J = 7.3$ Hz, 1H), 7.34–7.08 (m, 6H), 7.55 (d, $J = 7.9$ Hz, 1H), 7.73–7.64 (m, 1H), 8.11 (d, $J = 5.5$ Hz, 1H), 8.31 (s, 1H), 11.38 (s, 1H). Anal. Calcd for $C_{25}H_{22}ClN_7OS$ (%): C, 59.58; H, 4.40; N, 19.45. Found (%): C, 59.51; H, 4.39; N, 19.52.

5.8.18. (*E*)-4-(2-(2-((1-(3-Chlorobenzyl)-1*H*-benzo[*d*]imidazol-2-yl)methylene)hydrazinyl)thieno[3,2-*d*]pyrimidin-4-yl)morpholine (**17c**)

This compound was obtained as white solid in 70% yield. m.p. 266–268 °C. ESI-MS m/z : 504.0 $[M + H]^+$, 525.8 $[M + Na]^+$. IR (KBr) cm^{-1} : 3438.0, 3246.1, 1573.2, 1539.9, 1486.8, 1442.0, 1353.7, 888.7, 789.4, 740.1. 1H NMR (300 MHz, DMSO- d_6) δ : 3.56 (s, 4H), 3.73 (d, $J = 4.0$ Hz, 4H), 6.20 (s, 2H), 7.23 (dd, $J_1 = 11.3$ Hz, $J_2 = 5.8$ Hz, 4H),

7.29 (d, $J = 6.8$ Hz, 1H), 7.38 (d, $J = 7.1$ Hz, 2H), 7.47 (d, $J = 4.9$ Hz, 1H), 7.75–7.57 (m, 1H), 8.11 (d, $J = 5.5$ Hz, 1H), 8.31 (s, 1H), 11.42 (s, 1H). Anal. Calcd for $C_{25}H_{22}ClN_7OS$ (%): C, 59.58; H, 4.40; N, 19.45. Found (%): C, 59.51; H, 4.41; N, 19.51.

5.8.19. (*E*)-4-(2-(2-((1-(4-Chlorobenzyl)-1H-benzo[d]imidazol-2-yl)methylene)hydrazinyl)thieno[3,2-d]pyrimidin-4-yl)morpholine (**17d**)

This compound was obtained as pale yellow solid in 69% yield. m.p. 265–267 °C. ESI-MS m/z : 504.2 $[M + H]^+$. IR (KBr) cm^{-1} : 3429.2, 3211.7, 2966.1, 2852.4, 1578.5, 1540.0, 1443.5, 1367.7, 1177.3, 1014.2, 898.1, 788.7, 740.3. 1H NMR (300 MHz, DMSO- d_6) δ : 3.61 (d, $J = 4.3$ Hz, 4H), 3.74 (d, $J = 4.4$ Hz, 4H), 6.17 (s, 2H), 7.28–7.20 (m, 3H), 7.36 (d, $J = 8.5$ Hz, 2H), 7.42 (d, $J = 8.5$ Hz, 2H), 7.54–7.47 (m, 1H), 7.66 (dd, $J_1 = 5.9$ Hz, $J_2 = 3.0$ Hz, 1H), 8.12 (d, $J = 5.5$ Hz, 1H), 8.30 (s, 1H), 11.43 (s, 1H). Anal. Calcd for $C_{25}H_{22}ClN_7OS$ (%): C, 59.58; H, 4.40; N, 19.45. Found (%): C, 59.54; H, 4.37; N, 19.49.

5.8.20. (*E*)-4-(2-(2-((1-(4-*tert*-butylbenzyl)-1H-benzo[d]imidazol-2-yl)methylene)hydrazinyl)thieno[3,2-d]pyrimidin-4-yl)morpholine (**17e**)

This compound was obtained as light yellow solid in 61% yield. m.p. 253–255 °C. ESI-MS m/z : 526.5 $[M + H]^+$, 548.5 $[M + Na]^+$, 565.3 $[M + K]^+$. IR (KBr) cm^{-1} : 3432.7, 2963.1, 1576.5, 1544.9, 1361.0, 1184.6, 744.9. 1H NMR (300 MHz, DMSO- d_6) δ : 1.19 (s, 9H), 3.53 (s, 4H), 3.71 (d, $J = 4.2$ Hz, 4H), 6.15 (s, 2H), 7.22 (dd, $J_1 = 7.9$ Hz, $J_2 = 4.5$ Hz, 3H), 7.31 (s, 4H), 7.50 (d, $J = 8.1$ Hz, 1H), 7.64 (dd, $J_1 = 6.1$ Hz, $J_2 = 2.7$ Hz, 1H), 8.12 (d, $J = 5.5$ Hz, 1H), 8.30 (s, 1H), 11.44 (s, 1H). Anal. Calcd for $C_{29}H_{31}N_7OS$ (%): C, 66.26; H, 5.94; N, 18.65. Found (%): C, 66.19; H, 5.91; N, 18.67.

5.8.21. (*E*)-4-(2-(2-((1-(2,3-Dichlorobenzyl)-1H-benzo[d]imidazol-2-yl)methylene)hydrazinyl)thieno[3,2-d]pyrimidin-4-yl)morpholine (**17f**)

This compound was obtained as pale yellow solid in 71% yield. m.p. 296–298 °C. ESI-MS m/z : 538.0 $[M + H]^+$. IR (KBr) cm^{-1} : 3425.9, 2964.8, 2854.8, 1569.7, 1537.8, 1363.2, 1179.9, 788.0, 743.9. 1H NMR (300 MHz, DMSO- d_6) δ : 3.64 (s, 4H), 3.74 (d, $J = 3.8$ Hz, 4H), 6.27 (s, 2H), 7.34–7.17 (m, 6H), 7.54 (d, $J = 8.1$ Hz, 1H), 7.70 (d, $J = 7.9$ Hz, 1H), 8.11 (d, $J = 5.4$ Hz, 1H), 8.30 (d, $J = 5.1$ Hz, 1H), 11.34 (s, 1H). Anal. Calcd for $C_{25}H_{21}Cl_2N_7OS$ (%): C, 55.76; H, 3.93; N, 18.21. Found (%): C, 55.71; H, 3.92; N, 18.26.

5.9. Preparation of 2-(2-chloro-4-morpholinethieno[3,2-d]pyrimidin-6-yl)propan-2-ol (**18**)

To a suspension of 2-chloro-4-morpholine-4-yl-thieno[3,2-d]pyrimidine (20 g, 0.078 mol) in dry THF (500 mL) at -78 °C was added a 2.5 M solution of *n*-BuLi in hexane (56 mL, 0.14 mol). After stirring for 1 h, dry acetone (8.5 mL, 0.12 mol) was added. The reaction mixture was stirred for 2 h at -78 °C and then warmed slowly to room temperature. After a further 2 h at room temperature the mixture poured onto ice/water yielding a yellow precipitate. This was collected by filtration and dried to yield the title compound (20 g, 83%). m.p. 174–176 °C. ESI-MS m/z : 313.2 (Cl = 35), 315.1 (Cl = 37) $[M + H]^+$. 1H NMR (300 MHz, DMSO- d_6) δ : 1.57 (s, 6H), 3.75 (s, 4H), 3.90 (s, 4H), 5.95 (s, 1H), 7.22 (s, 1H).

5.10. Preparation of 2-(2-hydrazinyl-4-morpholinethieno[3,2-d]pyrimidin-6-yl)propan-2-ol (**19**)

According to the procedure used to prepare **13**, starting from **18**, key intermediate **19** was obtained as an off-white solid. Yield: 79%. m.p. 92–93 °C. ESI-MS m/z : 340.1 $[M + H]^+$. 1H NMR (300 MHz, DMSO- d_6) δ : 1.53 (s, 6H), 3.71 (s, 4H), 3.80 (s, 4H), 4.05 (s, 2H), 5.71 (s, 1H), 6.94 (s, 1H), 7.42 (s, 1H).

5.11. General procedure for preparation of compounds **20c**–**20k** and **20p**

They were prepared in a similar procedure as described for **15a**–**15o** and **17a**–**17f**. According to the procedure used to prepare **15a**–**15o** and **17a**–**17f**, starting from **14c**–**14k** or **14p**, compounds **20c**–**20k** and **20p** were obtained.

5.11.1. (*E*)-2-(2-(2-((1-(3-Chlorobenzyl)-1H-indol-3-yl)methylene)hydrazinyl)-4-morpholinethieno[3,2-d]pyrimidin-6-yl)propan-2-ol (**20c**)

This compound was obtained as light yellow solid in 74% yield. m.p. 233–234 °C. ESI-MS m/z : 561.1 $[M + H]^+$. IR (KBr) cm^{-1} : 3406.3, 2973.8, 2855.0, 1578.2, 1516.7, 1382.2, 1275.1, 1169.6, 888.2, 745.7. 1H NMR (300 MHz, DMSO- d_6) δ : 1.56 (s, 6H), 3.80 (d, $J = 4.3$ Hz, 4H), 3.96 (s, 4H), 5.45 (s, 2H), 5.75 (s, 1H), 7.00 (s, 1H), 7.27–7.09 (m, 3H), 7.34 (dd, $J_1 = 13.2$ Hz, $J_2 = 7.1$ Hz, 3H), 7.49 (d, $J = 8.0$ Hz, 1H), 7.82 (s, 1H), 8.26 (s, 1H), 8.50 (d, $J = 7.6$ Hz, 1H), 10.47 (s, 1H). Anal. Calcd for $C_{29}H_{29}ClN_6O_2S$ (%): C, 62.08; H, 5.21; N, 14.98. Found (%): C, 62.04; H, 5.19; N, 15.02.

5.11.2. (*E*)-2-(2-(2-((1-(4-Chlorobenzyl)-1H-indol-3-yl)methylene)hydrazinyl)-4-morpholinethieno[3,2-d]pyrimidin-6-yl)propan-2-ol (**20d**)

This compound was obtained as off-white solid in 75% yield. m.p. 251–252 °C. ESI-MS m/z : 561.1 $[M + H]^+$. IR (KBr) cm^{-1} : 3418.2, 3224.3, 1554.8, 1511.0, 1381.4, 1169.6, 885.6, 743.1. 1H NMR (300 MHz, DMSO- d_6) δ : 1.56 (s, 6H), 3.79 (s, 4H), 3.95 (s, 4H), 5.43 (s, 2H), 5.75 (s, 1H), 7.00 (s, 1H), 7.22–7.07 (m, 2H), 7.26 (d, $J = 8.2$ Hz, 2H), 7.38 (d, $J = 8.3$ Hz, 2H), 7.46 (d, $J = 7.7$ Hz, 1H), 7.80 (s, 1H), 8.26 (s, 1H), 8.49 (d, $J = 7.5$ Hz, 1H), 10.45 (s, 1H). ^{13}C NMR (DMSO- d_6) δ : 164.41, 163.91, 158.78, 158.58, 137.61, 137.42, 136.81, 132.82, 131.30, 129.73(2C), 129.32(2C), 125.98, 123.39, 121.01, 118.73, 113.56, 111.05, 105.36, 100.99, 70.99, 66.82(2C), 49.20, 46.64(2C), 32.65(2C). Anal. Calcd for $C_{29}H_{29}ClN_6O_2S$ (%): C, 62.08; H, 5.21; N, 14.98. Found (%): C, 62.05; H, 5.19; N, 15.01.

5.11.3. (*E*)-2-(2-(2-((1-(2-Fluorobenzyl)-1H-indol-3-yl)methylene)hydrazinyl)-4-morpholinethieno[3,2-d]pyrimidin-6-yl)propan-2-ol (**20e**)

This compound was obtained as white solid in 77% yield. m.p. 218–220 °C. ESI-MS m/z : 568.4 $[M + Na]^+$. IR (KBr) cm^{-1} : 3442.4, 1632.5, 1543.4, 1511.4, 1382.5, 1171.8, 1116.7, 745.9. 1H NMR (300 MHz, DMSO- d_6) δ : 1.57 (s, 6H), 3.80 (s, 4H), 3.96 (s, 4H), 5.46 (s, 2H), 5.79 (s, 1H), 7.03 (s, 1H), 7.20 (d, $J = 8.4$ Hz, 4H), 7.60–7.49 (m, 3H), 7.86 (s, 1H), 8.28 (s, 1H), 8.51 (d, $J = 7.4$ Hz, 1H), 10.51 (s, 1H). Anal. Calcd for $C_{29}H_{29}FN_6O_2S$ (%): C, 63.95; H, 5.37; N, 15.43. Found (%): C, 63.89; H, 5.39; N, 15.48.

5.11.4. (*E*)-2-(2-(2-((1-(3-Fluorobenzyl)-1H-indol-3-yl)methylene)hydrazinyl)-4-morpholinethieno[3,2-d]pyrimidin-6-yl)propan-2-ol (**20f**)

This compound was obtained as white solid in 79% yield. m.p. 243–244 °C. ESI-MS m/z : 545.2 $[M + H]^+$. IR (KBr) cm^{-1} : 3428.8, 3223.5, 1556.3, 1510.9, 1379.5, 1174.1, 745.5. 1H NMR (300 MHz, DMSO- d_6) δ : 1.57 (s, 6H), 3.80 (s, 4H), 3.96 (s, 4H), 5.46 (s, 2H), 5.75 (s, 1H), 7.01 (s, 1H), 7.26–7.03 (m, 5H), 7.36 (dd, $J_1 = 14.0$ Hz, $J_2 = 8.1$ Hz, 1H), 7.49 (d, $J = 8.0$ Hz, 1H), 7.82 (s, 1H), 8.27 (s, 1H), 8.50 (d, $J = 7.4$ Hz, 1H), 10.46 (s, 1H). Anal. Calcd for $C_{29}H_{29}FN_6O_2S$ (%): C, 63.95; H, 5.37; N, 15.43. Found (%): C, 63.90; H, 5.35; N, 15.36.

5.11.5. (*E*)-2-(2-(2-((1-(4-Fluorobenzyl)-1H-indol-3-yl)methylene)hydrazinyl)-4-morpholinethieno[3,2-d]pyrimidin-6-yl)propan-2-ol (**20g**)

This compound was obtained as off-white solid in 73% yield. m.p. 225–227 °C. ESI-MS m/z : 545.2 $[M + H]^+$. IR (KBr) cm^{-1} : 3425.7, 3223.7, 1555.6, 1509.8, 1379.7, 1266.9, 1170.7, 742.6. 1H NMR (300 MHz, DMSO- d_6) δ : 1.56 (s, 6H), 3.80 (s, 4H), 3.94 (s, 4H), 5.49 (s, 2H), 5.74 (s, 1H), 7.00 (s, 1H), 7.40–7.06 (m, 6H), 7.50 (d, $J = 8.1$ Hz,

1H), 7.73 (s, 1H), 8.25 (s, 1H), 8.49 (d, $J = 7.6$ Hz, 1H), 10.45 (s, 1H). ^{13}C NMR (DMSO- d_6) δ : 164.44, 163.89, 158.75, 158.60, 137.46, 136.78, 131.24, 130.66, 130.58, 130.36, 130.31, 125.45, 123.43, 121.04, 118.80, 116.42, 116.11, 113.58, 110.83, 105.34, 100.99, 70.99, 66.81(2C), 48.85, 46.64(2C), 32.63(2C). Anal. Calcd for $\text{C}_{29}\text{H}_{29}\text{FN}_6\text{O}_2\text{S}$ (%): C, 63.95; H, 5.37; N, 15.43. Found (%): C, 63.89; H, 5.34; N, 15.49.

5.11.6. (*E*)-3-((3-((2-(6-(2-Hydroxypropan-2-yl)-4-morpholinothieno[3,2-*d*]pyrimidin-2-yl)hydrazono)methyl)-1*H*-indol-1-yl)methyl)benzotrile (**20h**)

This compound was obtained as light yellow solid in 73% yield. m.p. 232–234 °C. ESI-MS m/z : 552.1 $[\text{M} + \text{H}]^+$. IR (KBr) cm^{-1} : 3427.9, 3231.2, 1556.3, 1508.9, 1380.4, 1171.5, 746.3. ^1H NMR (300 MHz, DMSO- d_6) δ : 1.57 (s, 6H), 3.80 (s, 4H), 3.96 (s, 4H), 5.50 (s, 2H), 5.75 (s, 1H), 7.01 (s, 1H), 7.28–7.08 (m, 2H), 7.63–7.40 (m, 3H), 7.75 (d, $J = 7.8$ Hz, 2H), 7.84 (s, 1H), 8.28 (s, 1H), 8.51 (d, $J = 7.5$ Hz, 1H), 10.47 (s, 1H). Anal. Calcd for $\text{C}_{30}\text{H}_{29}\text{N}_7\text{O}_2\text{S}$ (%): C, 65.32; H, 5.30; N, 17.77. Found (%): C, 65.19; H, 5.28; N, 17.84.

5.11.7. (*E*)-4-((3-((2-(6-(2-Hydroxypropan-2-yl)-4-morpholinothieno[3,2-*d*]pyrimidin-2-yl)hydrazono)methyl)-1*H*-indol-1-yl)methyl)benzotrile (**20i**)

This compound was obtained as light yellow solid in 75% yield. m.p. 156–158 °C. ESI-MS m/z : 552.2 $[\text{M} + \text{H}]^+$, 574.2 $[\text{M} + \text{Na}]^+$. IR (KBr) cm^{-1} : 3420.7, 2973.4, 2855.5, 1667.7, 1578.8, 1517.4, 1384.5, 1275.9, 1168.9, 1115.1, 765.9, 746.2. ^1H NMR (300 MHz, DMSO- d_6) δ : 1.57 (s, 6H), 3.81 (s, 4H), 3.96 (s, 4H), 5.68 (s, 2H), 5.75 (s, 1H), 7.07–6.88 (m, 2H), 7.31–7.10 (m, 2H), 7.47 (dd, $J_1 = 13.8$ Hz, $J_2 = 7.3$ Hz, 2H), 7.61 (t, $J = 7.6$ Hz, 1H), 7.75 (s, 1H), 7.91 (d, $J = 7.5$ Hz, 1H), 8.27 (s, 1H), 8.54 (d, $J = 7.2$ Hz, 1H), 10.48 (s, 1H). Anal. Calcd for $\text{C}_{30}\text{H}_{29}\text{N}_7\text{O}_2\text{S}$ (%): C, 65.32; H, 5.30; N, 17.77. Found (%): C, 65.21; H, 5.28; N, 17.80.

5.11.8. (*E*)-2-(2-(2-((1-(2,4-Dichlorobenzyl)-1*H*-indol-3-yl)methylene)hydrazinyl)-4-morpholinothieno[3,2-*d*]pyrimidin-6-yl)propan-2-ol (**20j**)

This compound was obtained as off-white solid in 76% yield. m.p. 231–233 °C. ESI-MS m/z : 595.1 (Cl = 35), 597.1 (Cl = 37) $[\text{M} + \text{H}]^+$. IR (KBr) cm^{-1} : 3293.5, 3196.2, 2924.1, 2927.9, 2853.4, 1545.7, 1513.6, 1375.2, 1173.4, 1123.6, 741.2. ^1H NMR (300 MHz, DMSO- d_6) δ : 1.57 (s, 6H), 3.80 (s, 4H), 3.96 (s, 4H), 5.51 (s, 2H), 5.75 (s, 1H), 6.75 (d, $J = 8.4$ Hz, 1H), 7.01 (s, 1H), 7.27–7.11 (m, 2H), 7.34 (d, $J = 8.3$ Hz, 1H), 7.41 (d, $J = 7.6$ Hz, 1H), 7.70 (d, $J = 5.5$ Hz, 2H), 8.26 (s, 1H), 8.53 (d, $J = 6.7$ Hz, 1H), 10.47 (s, 1H). Anal. Calcd for $\text{C}_{29}\text{H}_{28}\text{Cl}_2\text{N}_6\text{O}_2\text{S}$ (%): C, 58.49; H, 4.74; N, 14.11. Found (%): C, 58.42; H, 4.71; N, 13.97.

5.11.9. (*E*)-2-(2-(2-((1-(2,6-Dichlorobenzyl)-1*H*-indol-3-yl)methylene)hydrazinyl)-4-morpholinothieno[3,2-*d*]pyrimidin-6-yl)propan-2-ol (**20k**)

This compound was obtained as white solid in 73% yield. m.p. 241–243 °C. ESI-MS m/z : 595.4 (Cl = 35), 597.3 (Cl = 37) $[\text{M} + \text{H}]^+$. IR (KBr) cm^{-1} : 3422.1, 2970.1, 1550.5, 1510.5, 1377.8, 1172.3, 744.6. ^1H NMR (300 MHz, DMSO- d_6) δ : 1.57 (s, 6H), 3.80 (s, 4H), 3.96 (s, 4H), 5.58 (s, 2H), 5.75 (s, 1H), 6.60 (d, $J = 7.7$ Hz, 1H), 7.01 (s, 1H), 7.33–7.08 (m, 3H), 7.41 (d, $J = 7.7$ Hz, 1H), 7.58 (d, $J = 8.0$ Hz, 1H), 7.73 (s, 1H), 8.26 (s, 1H), 8.54 (d, $J = 7.1$ Hz, 1H), 10.48 (s, 1H). Anal. Calcd for $\text{C}_{29}\text{H}_{28}\text{Cl}_2\text{N}_6\text{O}_2\text{S}$ (%): C, 58.49; H, 4.74; N, 14.11. Found (%): C, 58.39; H, 4.71; N, 14.18.

5.11.10. (*E*)-2-(2-(2-((1-(2,3-Dichlorobenzyl)-1*H*-indol-3-yl)methylene)hydrazinyl)-4-morpholinothieno[3,2-*d*]pyrimidin-6-yl)propan-2-ol (**20p**)

This compound was obtained as off-white solid in 75% yield. m.p. 243–245 °C. ESI-MS m/z : 595.0 (Cl = 35), 597.1 (Cl = 37)

$[\text{M} + \text{H}]^+$. IR (KBr) cm^{-1} : 3225.7, 2972.1, 1578.7, 1553.3, 1508.1, 1377.6, 1174.6, 771.3, 744.8. ^1H NMR (300 MHz, DMSO- d_6) δ : 1.57 (s, 6H), 3.81 (d, $J = 4.3$ Hz, 4H), 3.96 (d, $J = 4.2$ Hz, 4H), 5.58 (s, 2H), 5.75 (s, 1H), 6.60 (d, $J = 7.6$ Hz, 1H), 7.01 (s, 1H), 7.28–7.15 (m, 3H), 7.41 (d, $J = 7.4$ Hz, 1H), 7.58 (d, $J = 7.8$ Hz, 1H), 7.73 (s, 1H), 8.26 (s, 1H), 8.54 (d, $J = 7.0$ Hz, 1H), 10.48 (s, 1H). ^{13}C NMR (DMSO- d_6) δ : 164.41, 163.92, 158.79, 158.58, 138.62, 137.65, 136.65, 132.85, 131.37, 130.44, 130.33, 129.20, 127.39, 125.87, 123.50, 121.22, 118.73, 113.93, 110.93, 105.40, 101.00, 70.99, 66.82(2C), 48.37, 46.64(2C), 32.65(2C). Anal. Calcd for $\text{C}_{29}\text{H}_{28}\text{Cl}_2\text{N}_6\text{O}_2\text{S}$ (%): C, 58.49; H, 4.74; N, 14.11. Found (%): C, 58.42; H, 4.72; N, 14.17.

5.12. Cytotoxicity assay *in vitro*

The cytotoxic activities of compounds (**15a–15o**, **17a–17f**, **20c–20k**, **20p**) were evaluated with H460, HT-29, MDA-MB-231, U87MG and H1975 cell lines by the standard MTT assay *in vitro*, with compound **5**, PAC-1 and GDC-0941 as the positive controls. The most promising compound **15f** was further evaluated against four cancer cell lines A549, H226, HepG2 and SGC-7901. The cancer cell lines were cultured in minimum essential medium (MEM) supplement with 10% fetal bovine serum (FBS).

Approximately 4×10^3 cells, suspended in MEM medium, were plated onto each well of a 96-well plate and incubated in 5% CO_2 at 37 °C for 24 h. The test compounds at indicated final concentrations were added to the culture medium and the cell cultures were continued for 72 h. Fresh MTT was added to each well at a terminal concentration of 5 $\mu\text{g}/\text{mL}$ and incubated with cells at 37 °C for 4 h. The formazan crystals were dissolved in 100 μL DMSO each well, and the absorbency at 492 nm (for absorbance of MTT formazan) and 630 nm (for the reference wavelength) was measured with the ELISA reader. All of the compounds were tested three times in each of the cell lines. The results expressed as IC_{50} (inhibitory concentration 50%) were the averages of three determinations and calculated by using the Bacus Laboratories Incorporated Slide Scanner (Bliss) software.

5.13. 3D-QSAR on H460 cell line

5.13.1. Data set

In this study, *in vitro* cytotoxic data against H460 cells were selected to construct the 3D-QSAR models, Table 1 list their structures and biological data. For CoMFA and CoMSIA analysis, 31 compounds with determinate IC_{50} values of H460 cell line were employed and their IC_{50} values were converted to pIC_{50} values according to the following formula:

$$\text{pIC}_{50} = \lg \frac{1}{\text{IC}_{50}}$$

5.13.2. Structure optimization and alignment

Construction and optimization of the compounds, CoMFA and CoMSIA modeling were all performed by the molecular modeling software SYBYL 6.91 (TRIPOS Associates Inc.) on Silicon Graphics workstation. The alignment of the molecules was derived by using SKETCH in SYBYL. Energy minimization were performed using Tripos force field and conjugate gradient method with a convergence criterion of 0.05 kcal/(mol·Å). Charges were calculated by the Gasteiger-hückler method in the software. Subsequently, all compounds were aligned using a 2-hydrazinyl-4-morpholinothieno[3,2-*d*]pyrimidine nucleus as a template, which is a common substructure in all molecules and the minimum scaffold required for active molecules, and compound **15f** with the highest pIC_{50} value was chosen as the template molecule [**21–22**].

5.13.3. CoMFA and CoMSIA studies

CoMFA calculation was carried out using default values. The steric (Lennard-Jones) and electrostatic (Coulomb) fields were calculated at each intersection on the regularly spaced grid. 3D cubic lattice with grid spacing of 2 Å and extending to 4 Å beyond the aligned molecules in all directions was used. Steric and electrostatic fields energies were calculated using a sp^3 carbon as the steric probe atom and +1 charge (default probe atom in SYSL) for the electrostatic probe with the cutoff energy of 30 kcal/mol.

CoMSIA similarity index descriptors were derived using the same lattice box as that used in CoMFA calculations. The standard settings were used in CoMSIA to calculate five different fields viz. steric, electrostatic, hydrophobic, acceptor and donor. The default value of 0.3 was used as the attenuation factor (R). The statistical evaluation for the CoMSIA analyses were performed in the same way as described for CoMFA.

5.13.4. Partial least squares (PLS) analysis

The CoMFA or CoMSIA descriptors were used as independent variables and pIC_{50} values as dependant variables in partial least square regression analysis. SAMPLS leave-one-out (LOO) Cross-validated PLS was performed to determine the optimal number of components to be used in the subsequent final analysis. Column filtering value was set 2.0 kcal/mol by omitting those lattice points those energy variation is below this threshold to improve the signal-to-noise ratio. Finally, no-cross-validated analysis was performed and employed to analyze the result of the CoMFA and CoMSIA models [22–23]. The predictive ability of the models is expressed by conventional correlation coefficient r^2 value, which is analogous to cross-validated r^2 (q^2). The cross-validated coefficient q^2 (or r^2) was evaluated as:

$$q^2 = 1 - \frac{\sum (Y_{\text{pred}} - Y_{\text{exp}})^2}{\sum (Y_{\text{exp}} - Y_{\text{mean}})^2}$$

where Y_{pred} , Y_{exp} , Y_{mean} are the predicted, experimental, and mean values of the pIC_{50} , respectively.

The standard error of estimate SE and the Fisher test F value were also derived to evaluate the predictive quality of the models.

Acknowledgments

We thank professor Maosheng Cheng and Dr Jian Wang for offering help in 3D-QSAR analysis. This work was supported by a grant from National S & T Major Project (No. 2009ZX09301-012) and National Natural Science Foundation of China (NSFC No. 21002065).

Appendix A. Supplementary material

Supplementary data related to this article can be found at <http://dx.doi.org/10.1016/j.ejmech.2012.09.002>.

References

- [1] <http://www.who.int/mediacentre/factsheets/fs297/en/> (WHO Media Centre Cancer Feb 8, 2012, last accessed: 26.03.12).
- [2] M. Lindvall, C. McBride, M. McKenna, T.G. Gesner, A. Yabannavar, K. Wong, S. Lin, A. Walter, C.M. Shafer, ACS Med. Chem. Lett. 2 (2011) 720–723.
- [3] Y. Ni, A. Gopalsamy, D. Cole, Y. Hu, R. Denny, M. Lpek, J. Liu, J. Lee, J.P. Hall, M. Luong, J.B. Telliez, L.L. Lin, Bioorg. Med. Chem. Lett. 21 (2011) 5952–5956.
- [4] T.P. Heffron, M. Berry, G. Castanedo, C. Chang, I. Chuckowree, J. Dotson, A. Folkes, J. Gunzner, J.D. Lesnick, C. Lewis, S. Mathieu, J. Nonomiya, A. Olivero, J. Pang, D. Peterson, L. Salphati, D. Sampath, S. Sideris, D.P. Sutherland, V. Tsui, N.C. Wan, S. Wang, S. Wong, B. Zhu, Bioorg. Med. Chem. Lett. 20 (2010) 2408–2411.
- [5] D.P. Sutherland, D. Sampath, M. Berry, G. Castanedo, Z. Chang, I. Chuckowree, J. Dotson, A. Folkes, L. Friedman, R. Goldsmith, T. Heffron, L. Lee, J. Lesnick, C. Lewis, S. Mathieu, J. Nonomiya, A. Olivero, J. Pang, W.W. Prior, L. Salphati, S. Sideris, Q. Tian, V. Tsui, N.C. Wan, S. Wang, C. Wiesmann, S. Wong, B. Zhu, J. Med. Chem. 53 (2010) 1086–1097.
- [6] N.S. Shetty, R.S. Lamani, I.A.M. Khazi, J. Chem. Sci. 121 (2009) 301–307.
- [7] A.B.A. El-gazzar, H.A.R. Hussein, H.N. Hafez, Acta Pharm. 57 (2007) 395–411.
- [8] A.J. Folkes, K. Ahmadi, W.K. Alderton, S. Alix, S.J. Baker, G. Box, I.S. Chuckowree, P.A. Clarke, P. Depledge, S.A. Eccles, L.S. Friedman, A. Hayes, T.C. Hancox, A. Kugendradas, L. Lensun, P. Moore, A.G. Olivero, J. Pang, S. Patel, G.H. Pergl-Wilson, F.I. Raynaud, A. Robson, N. Saghir, L. Salphati, S. Sohal, M.H. Ultsch, M. Valenti, H.J. Wallweber, N.C. Wan, C. Wiesmann, P. Workman, A. Zhyvoloup, M.J. Zvelebil, S.J. Shuttleworth, J. Med. Chem. 51 (2008) 5522–5532.
- [9] T.T. Junttila, R.W. Akita, K. Parsons, C. Fields, G.D. Lewis Phillips, L.S. Friedman, D. Sampath, M.X. Sliwkowski, Cancer Cell 15 (2009) 429–440.
- [10] D. Sarker, R. Kristeleit, K.E. Mazina, J.A. Ware, Y. Yan, M. Dresser, M.K. Derynck, J. De-Bono, J. Clin. Oncol. 27 (15S) (2009) 3538 (Meeting Abstracts).
- [11] P.J. Rohan, P. Davis, C.A. Moskaluk, M. Kearns, H. Krutzsch, U. Siebenlist, K. Kelly, Science 259 (1993) 1763–1766.
- [12] K.A. Menear, S. Gomez, K. Malagu, Bioorg. Med. Chem. 19 (2009) 5898–5901.
- [13] G. Zhang, Y. Liu, S. Wang, C. Zhou, Q. Huang, P. Gong, Arch. Pharm. Chem. Life Sci. 345 (2012) 49–56.
- [14] G.G. Zhang, Y.J. Liu, X.G. Ma, H. Dong, J. Li, P. Gong, Chin. Chem. Lett. 22 (2011) 1223–1225.
- [15] W. Guo, S.H. Wu, L. Wang, R. Wang, X. Wei, J. Liu, B. Fang, Mol. Cancer Ther. 8 (2009) 441–448.
- [16] D. Kumar, N.M. Kumar, K.H. Chang, R. Gupta, K. Shah, Bioorg. Med. Chem. Lett. 21 (2011) 5897–5900.
- [17] D. Kumar, N.M. Kumar, S. Ghosh, K. Shah, Bioorg. Med. Chem. Lett. 22 (2012) 212–215.
- [18] K.K. Roy, S. Singh, S.K. Sharma, R. Srivastava, V. Chaturvedi, A.K. Saxena, Bioorg. Med. Chem. Lett. 21 (2011) 5589–5593.
- [19] C. Garino, S. Ghiani, R. Gobetto, C. Nervi, L. Salassa, G. Croce, M. Milanese, E. Rosenberg, J.B. Alexander Ross, Eur. J. Inorg. Chem. 2006 (2006) 2885–2893.
- [20] T.H. Quang, T.T. Ha, C.V. Minh, P.V. Kiem, H.T. Huong, N.T.T. Ngan, N.X. Nhiem, N.H. Tung, B.H. Tai, D.T.T. Thuy, S.B. Song, H. Kang, Y.H. Kim, Bioorg. Med. Chem. 19 (2011) 2625–2632.
- [21] R. Cao, X. Guan, B. Shi, Z. Chen, Z. Ren, W. Peng, H. Song, Eur. J. Med. Chem. 45 (2010) 2503–2515.
- [22] A. Politi, S. Durdagi, P. Moutevelis-Minakakis, G. Kokotos, M.G. Papadopoulos, T. Mavromoustakos, Eur. J. Med. Chem. 44 (2009) 3703–3711.
- [23] A.Y. Shaw, C.Y. Chang, M.Y. Hsu, P.J. Lu, C.N. Yang, H.L. Chen, C.W. Lo, C.W. Shiau, M.K. Chern, Eur. J. Med. Chem. 45 (2010) 2860–2867.